[AMERICAN JOURNAL OF SCIENCE, VOL. 316, JUNE, 2016, P. 505–541, DOI 10.2475/06.2016.01]

American Journal of Science

JUNE 2016

THE EXHUMATION HISTORY OF THE EUROPEAN ALPS INFERRED FROM LINEAR INVERSION OF THERMOCHRONOMETRIC DATA

MATTHEW FOX*,**,†, FRÉDÉRIC HERMAN*,***, SEAN D. WILLETT*, AND STEFAN M. SCHMID*

ABSTRACT. **Thermochronometric data collected across the Alps over the last three decades allows for investigation of the evolution of this orogen, which is subject to changes in climate and geodynamics. Exhumation rates are inferred from the thermochronometric ages using a statistical inversion method based on the fact that the distance a sample traveled since closure is equal to the integral of the exhumation rate from the present day to the age of the sample. Exhumation rates are assumed to be spatially correlated but are free to vary through time. This results in the quantification of exhumation rates across the Alps, since 32 Ma, along with assessments of the quality of these inferences. We find that exhumation rates are initially fast in the internal arc of the Western Alps at rates up to 0.8 km/Myr at 30 Ma, decreasing at 20 Ma to 0.3 km/Myr to remain slow to the present. At the same time, around 20 Ma, rates across the External Crystalline Massifs of Western Alps increase to 0.6 km/Myr. We also find that the onset of high exhumation rates in the Tauern Window and the Lepontine Dome occurs at around 20 Ma, a time characterized by major reorganizations in the Alpine chain. A general increase in exhumation rates at around 5 Ma over the entire Alps is not confirmed. Instead we find that the Western Alps exhibit a 2 to 3 fold increase in exhumation rate over the last 2 Ma, during a recent event not seen further east, in spite of very similar topographic characteristics. We attribute this strong signal to detachment of the European slab in the Western Alps, combined with efficient glacial erosion.**

Keywords: European Alps, thermochronometry, exhumation rates, landscape evolution

INTRODUCTION

The European Alps are amongst the most extensively studied mountain belts on Earth, providing a wealth of information that allows us to better understand orogenic processes. However, the complexity of its evolution becomes more apparent as the amount of available information increases. Much of this complexity may be attributed to variations in plate convergence velocity, alternating pulses of compression and extension within the crust, changes in the mantle lithospheric configuration, and/or, the ongoing redistribution of mass through changes in the pattern of erosion and deposition. These factors are likely to lead to variations in the upward velocity of rocks with respect to surface of the Earth (for example, Ring and others, 1999), or exhumation rate as clarified in England and Molnar (1990). This contribution aims at quantifying exhumation rate in the Alps in space and time, which enables these

* Department of Earth Sciences, ETH, Zürich, Switzerland
** Present address: Department of Earth and Planetary Science, University of California, Berkeley, California, USA and Berkeley Geochronology Center, Berkeley, California, USA
*** Present address: Institute of Earth Science, University of Lausanne, Switzerland
† Corresponding author: matthew.fox@berkeley.edu

controlling factors to be disentangled and provides a better understanding of how they influence the evolution of the orogen.

Exhumation rates can be estimated using *in situ* thermochronometry (for example, Reiners and Brandon, 2006), as was first established within the Alps over 40 years ago (Clark and Jäger, 1969; Wagner and Reimer, 1972). At present, the Alpine thermochronometric dataset consists of approximately 3000 ages. Although many of these data have been compiled previously (for example, Hunziker and others, 1992; Fügenschuh and others, 1997; Vernon and others, 2008; Luth and Willingshofer, 2008), most analyses have focused on parts of the Alpine edifice only. The purpose of our study is to provide robust estimates of exhumation rates across the entire Alps from thermochronometric ages analyzed in a uniform and coherent way, and to relate these rates to known geodynamic processes. We employ a newly developed statistical method that relies on the fact that the depth to the 'closure isotherm' of a thermochronometric system can be described as the integral of exhumation rate, $\dot{e}$, from the cooling age to the present day. This permits a set of ages to be described as a linear system of equations related to exhumation rate that can be solved with a maximum likelihood approach (Fox and others, 2014a).

In the last three decades, many geological, petrological, sedimentological and geophysical investigations have been conducted in the European Alps. These have resulted in numerous syntheses dealing with tectonics and the overall geologic evolution of the system (for example, Schmid and others, 2004; Handy and others, 2010) as well as the role of tectonics and climate on setting exhumation rate (Willett, 2010). Our analysis allows us to evaluate what controls exhumation by comparing our estimates of exhumation rates in space and time to these existing observations. We begin by briefly highlighting what is known about geodynamical and climatic changes in the Alps that can potentially lead to variations in exhumation rate. This is followed by our unified analysis and inverse modeling of the complete Alpine dataset to produce a new, comprehensive model of exhumation of the Alps through time.

SETTING

European-Adriatic Collision

Alpine tectonics have been summarized in many publications (for example, Pfiffner, 1992; Schmid and others, 1996, 2004); here we provide only a brief introduction to the structure and evolution of the European Alps. Figure 1 provides an overview of the main tectonic units.

The Alps formed as a result of the convergence between the European and Adriatic lithosphere, including intervening microcontinents and oceans (Trümpy, 1973, 1980, 1988; Stampfli and Marthaler, 1990; Stampfli and Marchant, 1997; Stampfli and others, 1998). Much of the convergence history, between 70 to 35 Ma, was dominated by subduction towards the south with continued underplating of rifted remnants of the Adria margin, intervening oceans and microcontinents, and finally the European margin (Escher and Beaumont, 1997; Beaumont and others, 1996), which led to nappe stacking. These nappes are grouped by structural position and paleogeographic parentage.

The Austroalpine Nappes consist of basement and sedimentary units derived from the Adriatic (or Apulian) margin, which were stacked during a first orogenic event ('Eoalpine') with dominant WNW vergence in the Cretaceous and are related to the closure of Neotethys. These units are currently only exposed in the Eastern Alps and their western tectonic front now runs across strike through eastern Switzerland. Basement units derived from the Adriatic margin preserved in the Western Alps (Sesia Zone and the Dent Blanche Nappe) have a very different history in that they were incorporated into the subduction zone together with oceanic units derived from the

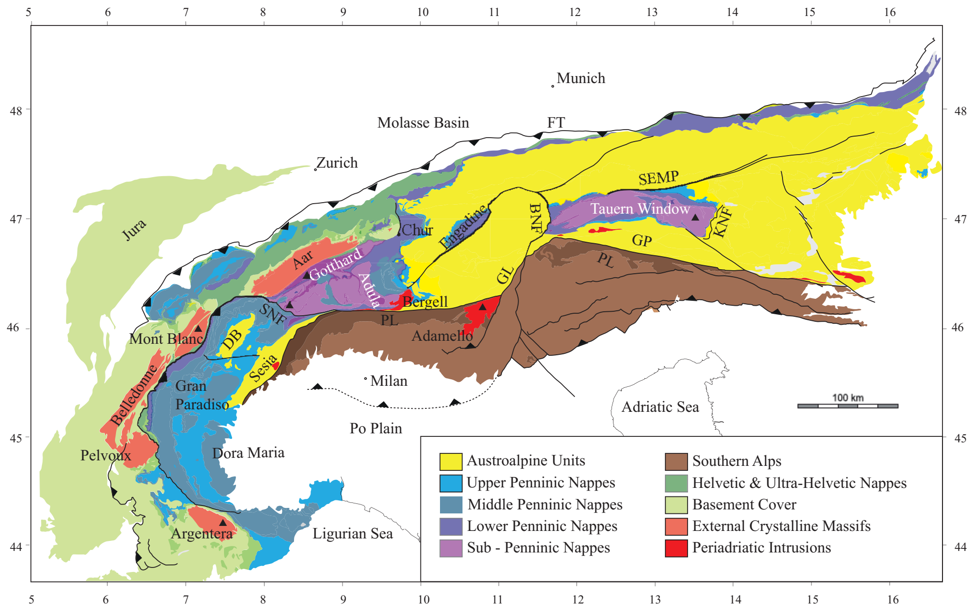

Fig. 1. Map of the European Alps showing the main features that are discussed throughout the text. BNF=Brenner Normal Fault, SNF=Simplon Normal Fault, SEMP=Salzachtal–Ennstal–Mariazell–Puchberg left–lateral strike–slip fault, GP=Gailtal-Pustertal right–lateral strike–slip, PF=Periadriatic Fault, GL=Giudicarie Line. The triangles show the locations of points considered in subsection of Results titled *Sensitivity of Exhumation Rates to the A Priori Model and Model Parameterization.* Modified from (Schmid and others, 2004).

Alpine Tethys in latest Cretaceous to Paleogene times, for example during a second orogenic event (Handy and others, 2010; Rubatto and others, 2011).

In the Tertiary, the Penninic and Subpenninic Nappes were progressively accreted to the previously formed Austroalpine Nappes during a second orogenic event, associated with dominant northwards vergence. Thereby units of more southerly provenance entered the subduction zone first. These Penninic and Subpenninic Nappes are presently exposed across the internal part of the Western Alps, within the Lepontine Dome, and within tectonic windows inside the Eastern Alps, such as the Engadine Window and Tauern Window (Schmid and others, 2004). The Piemont-Liguria ocean, the remnants of which constitute the Upper Penninic Nappes, was a narrow ocean that opened between the Eurasian and Adriatic-African plates in Jurassic times, and became subducted in latest Cretaceous to Early Eocene times (Dal Piaz and others, 2001; Handy and others, 2010). Subsequently a continental domain, the Briançonnais microcontinent, entered the subduction zone and eventually formed the Middle Penninic Nappes. In a third step, the Valais trough, a partly oceanic basin that opened between the Briançonnais and the European margin, became subducted by 42 to 40 Ma (Wiederkehr and others, 2008); its remnants form the Lower Penninic Nappes. The Subpenninic Nappes formed by accreted fragments of the distal margin of Europe and were the last to be accreted below Austroalpine and Penninic units. The structurally highest Subpenninic Nappes, for example, the Adula Nappe, reached peak-pressure conditions at approximately 38 Ma (Herwartz and others, 2011) while the lowest, for example, the Gotthard massif, lacking high-pressure overprint, reached peak temperature conditions as late as 18 Ma (Janots and others, 2009).

The low-grade or non-metamorphic Helvetic Nappes, consisting of detached sedimentary formations of European provenance formed between about 35 Ma and 20

Ma (Ramsay, 1981; Pfiffner, 1993). Their exposure is limited to large outcrops in Switzerland and narrow slivers across the Eastern and Western Alps.

The entrance of the more buoyant European margin into the subduction zone probably triggered slab breakoff (von Blanckenburg and Davies, 1995; Brouwer and others, 2004) and led to a change in the style of collision at 35 Ma; the Alps evolved into a doubly-vergent orogen with dominant southwards subduction of Europe persisting until today in the Western Alps. This new geometrical-kinematic framework was first inferred from structural geological mapping (Gerlach, 1869; Argand, 1911, 1916; Lugeon, 1914) and later from geophysical imaging techniques (Pfiffner and others, 1990; Nicolas and others, 1990; Marchant, ms, 1993; Escher and others, 1997; Schmid and Kissling, 2000; Lippitsch and others, 2003; Schmid and others, 2004; Diehl and others, 2009). The change to a doubly-vergent orogen is also marked by the onset of clastic sedimentation in the pro-foreland and retro-foreland basins (Karner and Watts, 1983; Mugnier and Vialon, 1986; Homewood and others, 1986; Allen and others, 1991; Sinclair, 1997) and the emplacement of the Bergell intrusion (Dal Piaz and others, 1988).

The model of a doubly-vergent wedge implies the development of retro- and pro-shear zones. The dominant retro-shear zone in the Alps from 35 Ma until 20 Ma, was the Periadriatic Line (Schmid and others, 1989), which separates the largely non-metamorphic Southern Alps from the Penninic (Western and Central Alps) or from the Austroalpine Nappes (Eastern Alps). This same model also predicts uplift of the former European continental margin within the pro-wedge (Beaumont and others, 1996). The European basement is exposed across the external arc of the Alps within the External Crystalline Massifs (ECMs), (that is, the Aar, Mont Blanc, Aiguilles Rouges, Belledonne, Pelvoux and Argentera massifs, fig. 1). The onset of exhumation of the ECMs has been estimated at 20 Ma (Leloup and others, 2005; Bigot-Cormier and others, 2006; Glotzbach and others, 2008; van der Beek and others, 2010).

The width of the orogenic wedge has changed through time. At about 20 Ma the main retro-shear zone stepped southwards into the Southern Alps (Schlunegger and Willett, 1999; Schlunegger and Simpson, 2002). The Southern Alps form an orogenic wedge with dominant southwards vergence. The cessation of faulting in the Southern Alps is dated to the end of the Miocene in the west, however further to the east it is ongoing (Roure and others, 1990; Fantoni and others, 2004). In the northern foreland of the Western and Central Alps, deformation stepped northwards to the Jura Mountains at about 12 Ma (Burkhard and Sommaruga, 1998) slowing or ending at around the end of the Miocene (for example, Burkhard, 1990; Sommaruga, 1999; Hindle, 2008; Willett and Schlunegger, 2010; von Hagke and others, 2012). However, slow deformation may still be occurring (Ustaszewski and Schmid, 2007; Rosenberg and Berger, 2009; Madritsch and others, 2010).

Major Extensional Structures

Orogen-parallel extension plays an important role in exhuming some parts of the Alps. In the Central Alps, the Simplon-Rhone Shear zone (fig. 1) represents a large right-lateral transtensional system with a major extensional detachment at the western margin of the Lepontine Dome (Mancktelow, 1992; Schmid and Kissling, 2000). The Simplon-Rhone shear zone separates amphibolite grade rocks in the Lepontine in the foot-wall from greenschist grade rocks in the hanging-wall (Steck and Hunziker, 1994). Deformation along the Simplon-Rhone shear zone began some 35 to 30 Myr ago under ductile conditions and has remained active until recent times (Steck and Hunziker, 1994; Campani and others, 2010a). In the Eastern Alps the main structures accommodating orogen-parallel extension are the Brenner and Katschberg normal faults, and the conjugate Salzachtal-Ennstal-Mariazell-Puchberg (SEMP) left-lateral and the Gailtal-Pustertal right-lateral (GP) strike-slip fault systems (Schmid and others, 2013), figure 1.

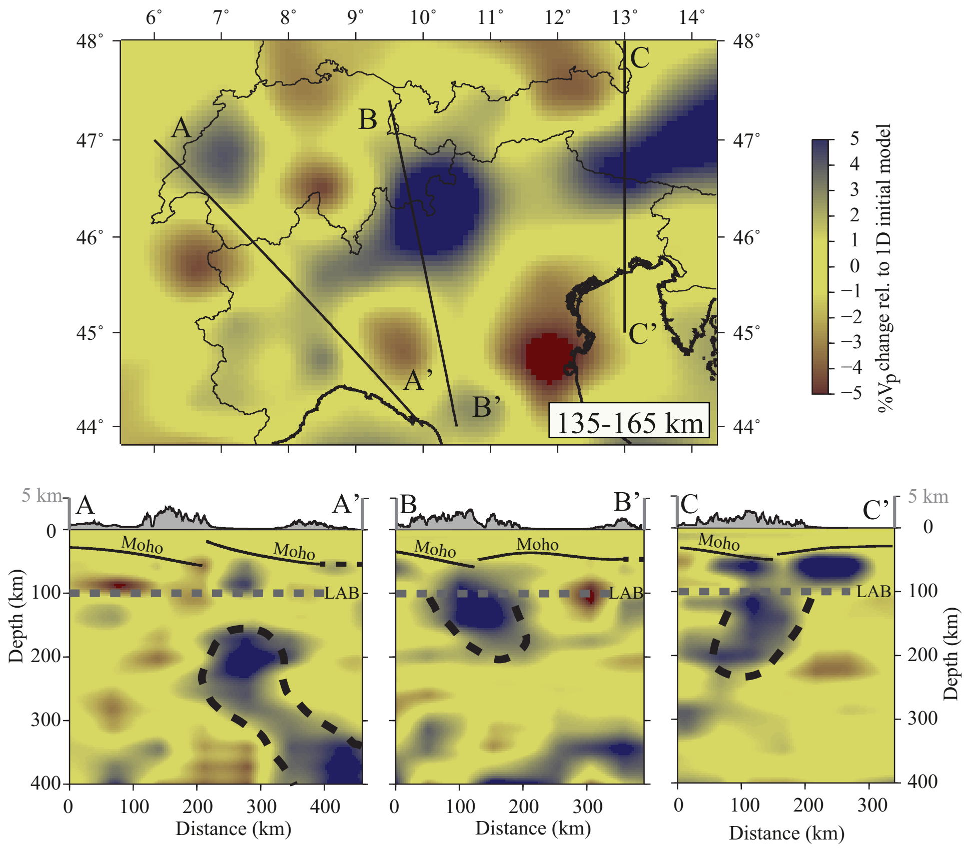

Fig. 2. Teleseismic tomographic model for the upper mantle below the Alps, plotted as a percent perturbation from a reference model (Lippitsch and others, 2003). The detached zone is seen as a slow anomaly below the Western Alps at a depth of 120 to 150 km. The southward dipping European slab is the fast anomaly below the central Alps. In the Eastern Alps there is a reversal in the polarity of subduction and the fast anomaly delineates the northward dipping Adriatic plate. At 180 km a fast anomaly is identified south east of the Western Alps and is interpreted as the detached European slab. The resolution does not permit the tip of the tear in the European slab to be identified. Above the Lithosphere Asthenosphere Boundary (LAB) the resolution of model is poor. The topography is shown in gray.

Orogen-parallel normal faulting, together with orogen-perpendicular shortening and erosion, assisted unroofing of the Tauern Window that cooled in Latest Oligocene to Early Miocene times (Luth and Willingshofer, 2008). Conjugate strike-slip faulting accommodated strain associated with lateral movement of the Eastern Alps with respect to the Central Alps, and has been active since the Oligocene (Ratschbacher and others, 1991b, 1991a; Plan and others, 2010; Wölfler and others, 2011).

Lithospheric Structure

Geophysical imaging suggests lithospheric scale differences between the Western, Central and Eastern Alps (fig. 2). Notably, a switch in the present-day subduction polarity located in the area of the Tauern Window has been proposed (Lippitsch and others, 2003; Kissling and others, 2006). Southwards subduction of Europe below the Alps is inferred to have remained active during and after the Miocene. However, at present the Adriatic plate that underlies the Eastern Alps dips in an almost opposite direction, that is to the NE (Mitterbauer and others, 2011). The transition to the present plate configuration probably occurred at ~20 Ma (Ustaszewski and others, 2008), while the effect of this transition on the surface dynamics remains unknown. Presently, the European plate below the Western Alps has been interpreted as being detached (fig. 2), and based on convergence rates and mantle tomography imaging, slab break-off likely occurred within the last 5 Myr (Lippitsch and others, 2003; Handy and others, 2010).

Present-day Shortening and Rock Uplift Rates

Present day convergence rates differ along strike of the Alps. The Western Alps are no longer undergoing contraction (Calais and others, 2002; Nocquet and Calais, 2004; Delacou and others, 2004; D'Agostino and others, 2008), however, the Eastern Alps continue to shorten at a rate of 2 mm/yr (D'Agostino and others, 2008). It is clear, however, that the present-day convergence velocities do not reflect the Tertiary average, neither in magnitude nor direction (Handy and others, 2010). The lack of present day convergence in the Western and Central Alps is surprising, particularly in light of ongoing rock uplift within this part of the Alps (Schlatter and others, 2005). Moreover, the Western Alps are characterized by ongoing extensional faulting within their core while compression prevails in the forelands to either side (Sue and others, 1999; Delacou and others, 2004; Selverstone, 2005; Champagnac and others, 2006).

Geophysical observations may provide mechanisms to account for this apparent discrepancy. Differences between observed and predicted gravity anomalies within the Western Alps led Lyon-Caen and Molnar (1989) to propose asthenospheric upwelling. Heterogeneities in mantle density, inferred from tomographic models, have also been used to infer the amount of topography that is dynamically supported by asthenospheric upwelling. Using this approach, Faccenna and Becker (2010); Boschi and others (2010) estimated up to 2 km of dynamic topography across the Western Alps, with respect to the Eastern Alps.

Changes in climate, and corresponding changes in erosional efficiency, have also been used to explain present day rock uplift rates. As a high latitude mountain belt, the Alps have been extensively affected by Pleistocene glaciations and enhanced erosion, which leads to isostatic rebound and increased rock uplift rate (Wittmann and others, 2007; Champagnac and others, 2007; Champagnac and others, 2009; Sternai and others, 2012). However, the response of the orogen to increased erosion depends on whether the orogen is active or not. During the Neogene, the Alps behaved as an active orogenic wedge, and changes in the erosion mechanisms, and the subsequent redistribution of mass would have led changes in the focus of rock uplift (Roe and others, 2003; Whipple and Meade, 2004; Stolar and others, 2007; Roe and others, 2008). Distinguishing erosion rate changes driven by climate change from those associated with tectonic activity is, therefore, not trivial in an active orogenic belt. However, if the Alps are not in a critically tapered state, the response to increased erosion will be easier to identify; the surrounding basins would be uplifted due to flexure only (Champagnac and others, 2008).

INDEPENDENT ESTIMATES OF EXHUMATION RATES

Sediment Budget Analyses

There has been significant work in quantifying the amount of Alpine derived material preserved in sedimentary basins surrounding the Alps and offshore (Kuhlemann and others, 2001, 2002; Kuhlemann and Kempf, 2002; Kuhlemann and others, 2006; Kuhlemann, 2007). For most of the Neogene, these data imply an average erosion rate of approximately 0.2 to 0.6 km/Myr (Kuhlemann, 2000). Most importantly, the sediment yield from the Alps suggests that erosion rates increased over the past ~5 Myr, which is consistent with global observations (Hay and others, 1988; Zhang and others, 2001; Molnar, 2004). In the Po Foreland Basin, where age control is best, this increase appears to have begun at 5.5 Ma (Willett and others, 2006). The reasons for this increase are much debated. It cannot be attributed solely to Plio-Pleistocene glaciation, which seems to have led to intensified glacial erosion at the middle Pleistocene-transition (Muttoni and others, 2003; Haeuselmann and others, 2007; Glotzbach and others, 2011; Valla and others, 2011). However, there are multiple sources of uncertainty associated with the analysis of sediment deposits. Temporal resolution is limited by poor stratigraphic age control in the depositional basin and spatial resolution relies on the reconstruction of past drainage systems. Moreover, the inability to quantify hiatuses leads to underestimations of the sedimentation rates (Sadler, 1999). This problem becomes even more apparent further back in time. Consequently, short-term rates are systematically faster than long-term rates (Sadler, 1999; Schumer and Jerolmack, 2009; Willenbring and Von Blanckenburg, 2010).

Detrital Thermochronology

The sedimentary basins neighboring the Alps also enable us to estimate exhumation rates through detrital thermochronological studies. The difference between stratigraphical age and cooling age, the 'lag-time', reflects the time required for the grain to travel from the closure depth to the depositional basin (Garver and others, 1999). If the time taken to transport eroded material from the source to the basin is negligible, the lag-time reflects erosion rate. Inferred rates vary from approximately 1 km/Myr since 17.5 Ma for the Central Alps to 0.5 km/Myr since 10 Ma for the Western Alps to 0.2 to 0.3 km/Myr for the slowest exhuming regions (Bernet and others, 2001, 2004, 2009; Glotzbach and others, 2011).

DATA USED IN THIS STUDY

Thermochronometric Data

The distribution of thermochronometric data across the Alps is highly varied (Fox and others, 2015). In general previous studies have focused in fast exhuming locations, such as the Mont Blanc area, the Lepontine Dome and the Tauern Window, figure 3. In addition, different thermochronometric systems were preferentially used in different locations. Note that we only consider Neogene ages of Alpine cooling and exhumation. Ages older than 35 Ma are not used for analysis, nor do we use crystallization ages recording pluton emplacement or formation ages due to brittle faulting and fluid flow.

In order to improve the consistency of the dataset and avoid the effects of anomalous ages, we exclude some reported ages from the analysis. Most of them are ages that are possibly affected by fluid flow, or thermal anomalies associated with Periadriatic Intrusions, and have been identified as such in the original publications. Apatite fission track (AFT) ages obtained with the population method have also been omitted from the analysis, where inconsistent with ages obtained using modern methods [see Gallagher and others (1998) for details on the limitations of the population method]. In addition, low uranium content in several samples makes AFT ages unreliable and such data have also been removed. Where measurement errors have not been reported, we assign a conservative uncertainty of 20 percent of the reported age. Ages obtained with high-temperature systems are associated with very low analytical error. However, this uncertainty does not represent the reproducibility of ages and hence we assign an uncertainty of 15 percent to such ages. A summary of the ages and typical values of closure depths are shown in table 1.

Heat Flow Data

For the Alps, a surface heat flux value of ~70 mW/m^2 (Clark Jr. and Niblett, 1956; Bodmer and Rybach, 1984; Lucazeau and Vasseur, 1989; Cermak, 1993) has been

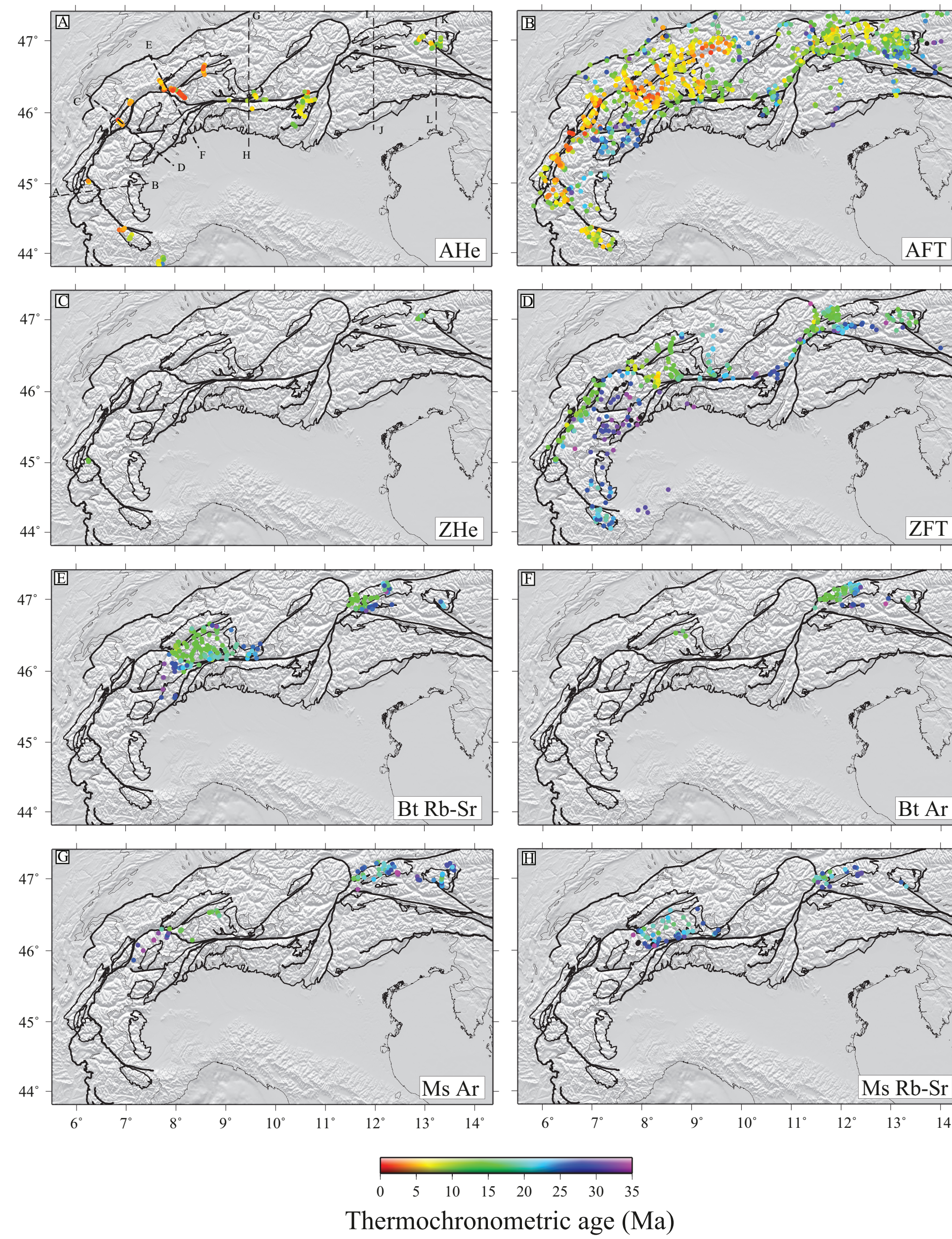

Fig. 3. Compilation of thermochronometric ages obtained using the following systems: (A) apatite (U-Th)/He; (B) apatite fission track; (C) zircon (U-Th)/He; (D) zircon fission track; (E) biotite Rb-Sr; (F) biotite K-Ar; (G) muscovite K-Ar; (H) muscovite Rb-Sr.

estimated, which corresponds to a present-day geothermal gradient of ~30 °C/km. This surface heat flux is poorly constrained across the Alps, however, and different parts of the chain could have very different values, varying between ~20 to 45 °C/km. In addition, these estimates do not include regions that are influenced by groundwater flow.

Table 1

The different thermochronometric systems used in the analysis. T_c is calculated using the diffusion parameters in the respective references with a cooling rate of 10 °C/Ma

System	N	Minimum age (Ma)	Maximum age (Ma)	Mean age (Ma)	T_c (°C)	Reference
AFT	1264	1.1	35.9	11.5	116	Ketcham and others (1999)
ZFT	426	5.4	35.9	19.7	232	Brandon and others (1998)
AHe	224	0.8	25.5	7.9	67	Farley (2000)
ZHe	13	12.5	19.1	14.8	183	Reiners and others (2004)
ArAr (mus)	91	9.21	35	23.6	380	Hames and Bowring (1994)
ArAr (bio)	84	12.7	35	20.3	348	Grove and Harrison (1996)
RbStr (mus)	96	24.2	22.95	24.2	420	Jenkin (1997)
RbStr (bio)	221	18.8	17.6	18.8	260	Jenkin (1997)
RbStr (mus)	96	24.2	22.95	24.2	420	Jenkin (1997)
RbStr (bio)	221	18.8	17.6	18.8	260	Jenkin (1997)

METHOD TO INFER EXHUMATION RATES FROM THERMOCHRONOMETRIC DATA

We use a method designed to efficiently convert thermochronometric data to exhumation rates (Fox and others, 2014a) that allows us to determine an exhumation rate function that is both variable in space and through time. The basis of the method is that for any single age, we define the 'closure depth', z_c (km) as the integral of exhumation rate, $\dot{e}$ (km/Myr), from the present day back to the cooling age,

$$\int_0^{\tau} \dot{e}\, dt = z_c \tag{1}$$

where τ is the cooling age. Therefore, if we are able to estimate z_c (km), an average exhumation rate over the time recorded by the age can be determined. Through the inclusion of multiple ages we are able to infer changes in exhumation rate through time because ages record exhumation rates over different time intervals. We first outline the steps taken to estimate z_c for a given age. We then show how we combine multiple ages to infer exhumation rates in space and through time.

Thermal Model and Closure Depths

Thermochronometric ages record the time elapsed since a sample cooled through a given temperature. In order to obtain closure depths, we require an estimate of the thermal structure of the crust at this time in the past (Dodson, 1973). The two key effects we need to capture are the perturbation of temperature by the surface topography and the vertical advection of heat by surface erosion and the upward motion of rock. We deal with each of these separately by decomposing the thermal field into two components (Turcotte and Schubert, 1982): an average temperature which varies with depth and time due to variations in exhumation, and a perturbation away from this average induced by the topography.

The estimate of the thermal structure of the crust through time introduces a large uncertainty to the analysis. The thermal model needs to be consistent with the measured present day heat flux. Unfortunately, a wide range of parameters influence the thermal structure of the crust in space and time and, as a consequence, a large number of thermal models are consistent with the present-day heat flux. To our advantage, the non–uniqueness of the problem can be greatly reduced by exploiting *a priori* information in the form of an average exhumation rate and an onset of exhumation. For simplicity, we also assume that there have been no variations in the thermal diffusivity or basal heat flux through time. We are left with the option of changing the initial geothermal gradient and associated basal heat flux to fit the measured surface heat flux.

The first component, the average thermal field, is calculated from the 1-D finite difference solution to the advection-diffusion equation for heat transfer to an isothermal boundary at the Earth's surface. We calibrate this average thermal model to the regional near surface geothermal gradient inferred from heat flow measurement (Clark and Niblett, 1956; Bodmer and Rybach, 1984; Lucazeau and Vasseur, 1989; Cermak, 1993). We set the upper boundary of the thermal model at 4 °C at 1475 m. The advective term in the heat equation, due to erosion, is determined using the *a priori* model. The basal heat flux and the initial condition of the thermal model are adjusted to provide present day surface heat flux values of $\sim$70 mW m^{-2}. We assume a thermal conductivity of 2.6 Wm^{-1}K^{-1}. Given the thermal conductivity and surface temperature we impose a basal heat flux at 90 km of 40 mW m^{-2} to provide a surface heat flow that is consistent with observations, that is 32 °C/km.

To evaluate a closure temperature for a specific thermochronometric age, a cooling rate at the time equivalent to the thermochronometric age is required. The material derivative of the transient average geotherm evaluated at the time in the past equivalent to the thermochronometric age provides cooling rate as a function of depth, which can be converted to closure temperature using Dodson's equation (Dodson, 1973). Therefore, an initial estimate of the closure depth is the depth where the temperature and the closure temperature are equal.

The second component, the perturbation away from this average temperature profile induced by the topography at the relevant time is also required to accurately estimate a specific closure depth. Initially, we reduce surface topography and surface temperature to perturbations of temperature on a horizontal plane located near the Earth's surface. Three components are required to calculate this temperature perturbation: (1) a digital elevation model, here we use a 90 m digital elevation model (Jarvis and others, 2006); (2) an estimate of the atmospheric lapse rate of 6 °C/km; (3) the near surface geothermal gradient determined from the average transient solution at the relevant time. Temperature perturbations on a plane at the surface can then be propagated downwards to a specific depth using a spectral method (Turcotte and Schubert, 1982; Stüwe and others, 1994; Mancktelow and Grasemann, 1997). In turn, the perturbation in temperature at a specific depth is converted to a perturbation in depth of a closure isotherm using the geothermal gradient at that depth determined from the average transient solution at the relevant time. We assume that the perturbation induced by the modern topography is representative of the perturbation at the time equivalent to the thermochronometric age, as detailed in Fox and others (2014a).

We illustrate the resulting closure elevations along six transects (locations shown in fig. 3A) across the Alpine chain (fig. 4).

Inverse Approach

By discretizing equation (1) into timesteps of uniform length, Δt, we can relate ages to closure depths, including depth uncertainty (ϵ), through,

$$\mathbf{A}\dot{\mathbf{e}} + \boldsymbol{\epsilon} = \mathbf{z}_c, \tag{2}$$

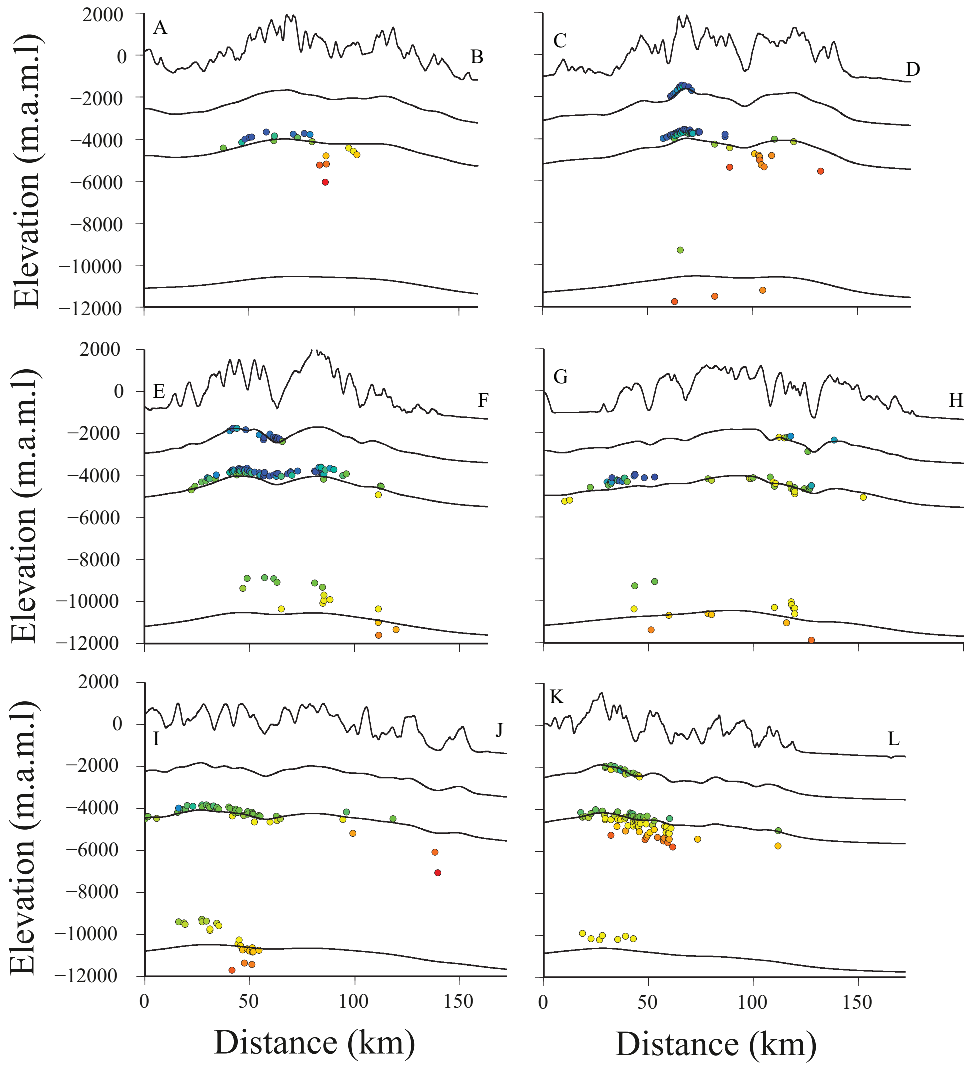

Fig. 4. Illustration of resulting closure elevations along six transects (see fig. 3A) across the Alpine chain. Uppermost solid black lines represent the topography, and the deeper solid black lines show the 'closure surfaces' for the AHe, AFT and ZFT systems, respectively. The latter represent the average perturbation caused by the present day topography for different thermochronometric systems. The colored circles show the elevation at which a sample begins to accumulate age, the colors reflecting the measured age, as provided in figure 3. The closure depth, z_c (km), is the distance between closure elevation and elevation at which the sample was collected.

where **A** is a matrix containing the ages, such that each row sums to the corresponding age, that is $M_i\Delta t + R_i = \tau_i$, where R_i is a remainder term. $\dot{\mathbf{e}}$ and $\mathbf{z_c}$ are vectors containing the exhumation rates and closure depths, respectively.

To solve these independent equations, we require that exhumation rate is correlated in space for a given time interval. This is imposed by defining an *a priori* covariance matrix for the exhumation rate and obtaining the maximum likelihood solution (Jackson, 1972; Tarantola and Valette, 1982). The covariance matrix for each time interval is constructed using the separation distance between the *i*th and *j*th data, x, and a spatial correlation function, $\rho(x)$,

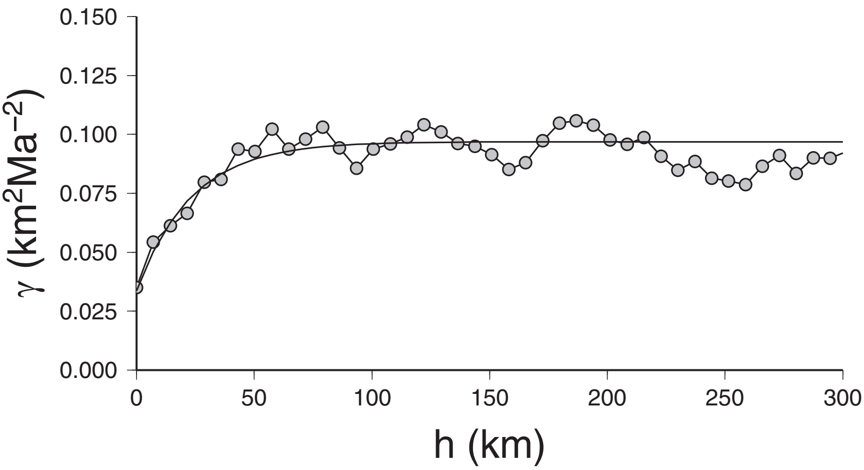

Fig. 5. Semi–variogram for the estimated mean exhumation rates. The black line is a modeled exponential correlation function with $\phi = 25$ km, $s = 0.06$ km^2 Myr^{-2} and $n = 0.03$ km^{2}Myr^{-2}. The number of pairs of ages used to calculate the variance in each population is more than ~30,000.

$$\mathbf{C}_{ij} = \sigma_{pr}^2 \delta_{ij} \rho(x), \qquad i,j \in [1,n]. \tag{3}$$

The *a priori* variance for the exhumation rate, σ_{pr}^2, serves primarily as a weighting factor for data uncertainty. The spatial correlation function $\rho(x)$, can be determined directly from the ages, however, quantitative correlations of exhumation rate are preferred as this allows ages obtained from multiple systems to be analyzed simultaneously. To obtain an estimate of time averaged exhumation rate, we divide z_c by τ for each age in the dataset.

Assuming exhumation rate varies smoothly in space, exhumation rate can be described as a spatial stochastic process, whereby points that are closer together in space are more likely to be similar. In turn, we quantify the correlation of this spatial stochastic process by calculating an empirical semi–variogram, γ, directly from the data. To this end, we calculate the separation distance and difference in exhumation rate between each pair of ages [that is, $(n - 1)^2$], and bin the differences according to the separation distance, h, using a bin size of 6 km and compute $\hat{\gamma}$ as,

$$\hat{\gamma}(h) = \frac{1}{2N(h)} \sum_{(i,j)\in N(h)} |\bar{\dot{e}}_i - \bar{\dot{e}}_j|^2, \tag{4}$$

where $N(h)$ is the number of pairs of ages within a particular bin, and $\bar{\dot{e}}$ is the average exhumation rate since a time equivalent to the age. The correlation function is then estimated by fitting a model that describes correlation as a function of separation distance to the empirical semi–variogram. We use an exponential model of the form,

$$\gamma(h) = s(1 - \exp(-h/\phi)) + \eta, \tag{5}$$

where η is the nugget effect, representing random variance, s is the sill parameter, where the variance remains constant with increasing separation distance and ϕ is the length scale parameter (fig. 5), which is equal to ~25 km.

This allows us to write the expected correlation between exhumation rates that are separated by a horizontal distance, u, as,

$$\rho(u) = \exp(-u/\phi). \tag{6}$$

This inferred correlation is then imposed in the model covariance matrix, equation (3).

It is assumed that exhumation rate does not correlate in time, so the matrices for each time interval can be combined, setting cross-terms to zero. The maximum likelihood estimate for the exhumation rate, or the *a posteriori* exhumation rate, is:

$$\dot{\mathbf{e}}_{\mathbf{po}} = \dot{\mathbf{e}}_{\mathbf{pr}} + \mathbf{CA}^T(\mathbf{ACA}^T + \mathbf{C}_\epsilon)^{-1}(\mathbf{z}_c - \mathbf{A}\dot{\mathbf{e}}_{\mathbf{pr}}), \tag{7}$$

where $\dot{e}_{pr}$ is the *a priori* expected value of the exhumation rate, used to reduce the model parameters to a zero expected value, and $\mathbf{C}_\epsilon$ is a diagonal matrix containing the estimated data uncertainty which we obtain from the analytical errors in the measurements. We calculate a parameter resolution matrix as,

$$\mathbf{R} = \mathbf{CA}^T(\mathbf{ACA}^T + \mathbf{C}_\epsilon)^{-1}\mathbf{A}. \tag{8}$$

This is integrated across the spatial dimension to obtain the temporal resolution values; if the integrated resolution is unity, the rates are perfectly resolved by the data within the specified time interval (Fox and others, 2014a).

RESULTS

The results of the inversion using the method described above are non-unique in the sense that decisions are made when setting up the model. We first present an inversion result as a series of maps based on a particular model configuration. As it is important to establish which features of the results are robust with respect to model parameterization and the *a priori* model, we evaluate the influence of changing these particular parameters on the *a posteriori* exhumation rate.

Exhumation Rates in Space and Time

We now present results that use our preferred *a priori* model. As previously discussed, a range of different exhumation rates are observed across the Alps, ranging from 0 to several km/Myr. We use an exhumation rate of 0.6 km/Myr for the *a priori* exhumation rates as this is representative of the average Alpine exhumation rate since 35 Ma. Furthermore, we use an *a priori* standard deviation of 0.1 km/Myr and a time-step length of 2 Myr.

Inversion result.—We now present our results by solving equation (7) and equation (8). Figures 6, 7, 8 and 9 present maps depicting exhumation rate for the last 32 Myr (top), along with maps that evaluate the temporal resolution (bottom). Also shown are the locations of the ages that are within a given time interval, plotted upon the temporal resolution. Before discussing the implications of these maps, we first establish the sensitivity of the results to the model configuration.

The difference between modeled ages and the predicted ages are shown in figure 10. Note that there is a tendency to under-predict ages. We attribute this feature to the fact that, in general, older ages have larger measurement uncertainties and hence are given less weight. Moreover, there are more ages collected from areas with higher exhumation rates.

Sensitivity of Exhumation Rates to the A Priori Model and Model Parameterization

Since the results presented in figure 6 to figure 9 represent one solution amongst a number of acceptable solutions using different parameterizations or *a priori* models, we perform a sensitivity study, figure 11. First, we assess the influence of Δt on the solution, investigating timestep lengths of 1 to 10 Myr. Second, we assess the role of the initial geothermal gradient. Finally, we vary the *a priori* variance, σ^2_{pr}.

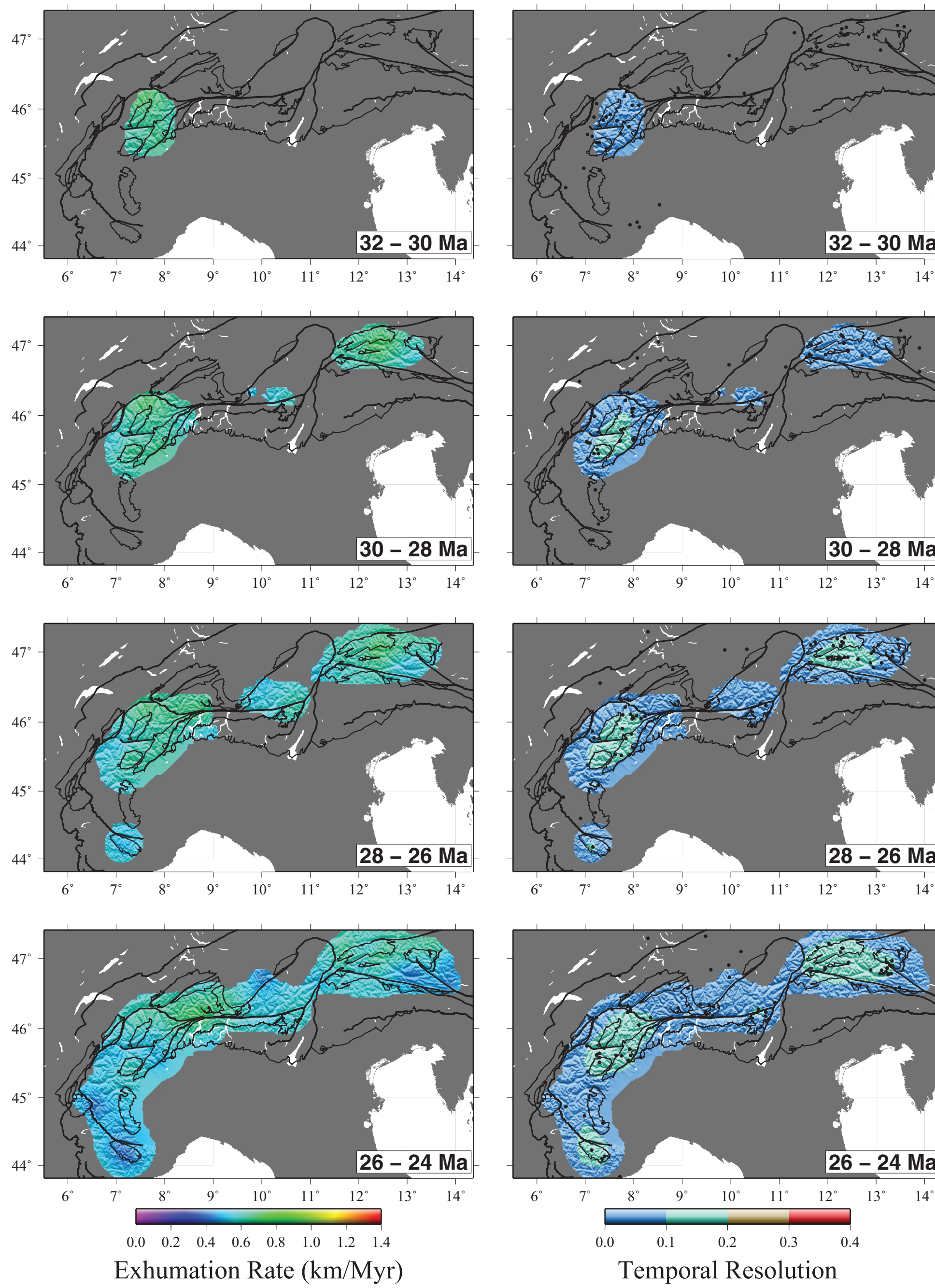

Fig. 6. Exhumation rates for the time intervals 32–30 Ma, 30–28 Ma, 28–26 Ma, and 26–24 Ma. Top panels: inferred exhumation rate in for time interval indicated. Bottom panel: temporal resolution; gray regions have a temporal resolution of less than 0.1, a resolution value of unity indicates perfect temporal resolution; black circles indicate locations of age data falling within the time interval.

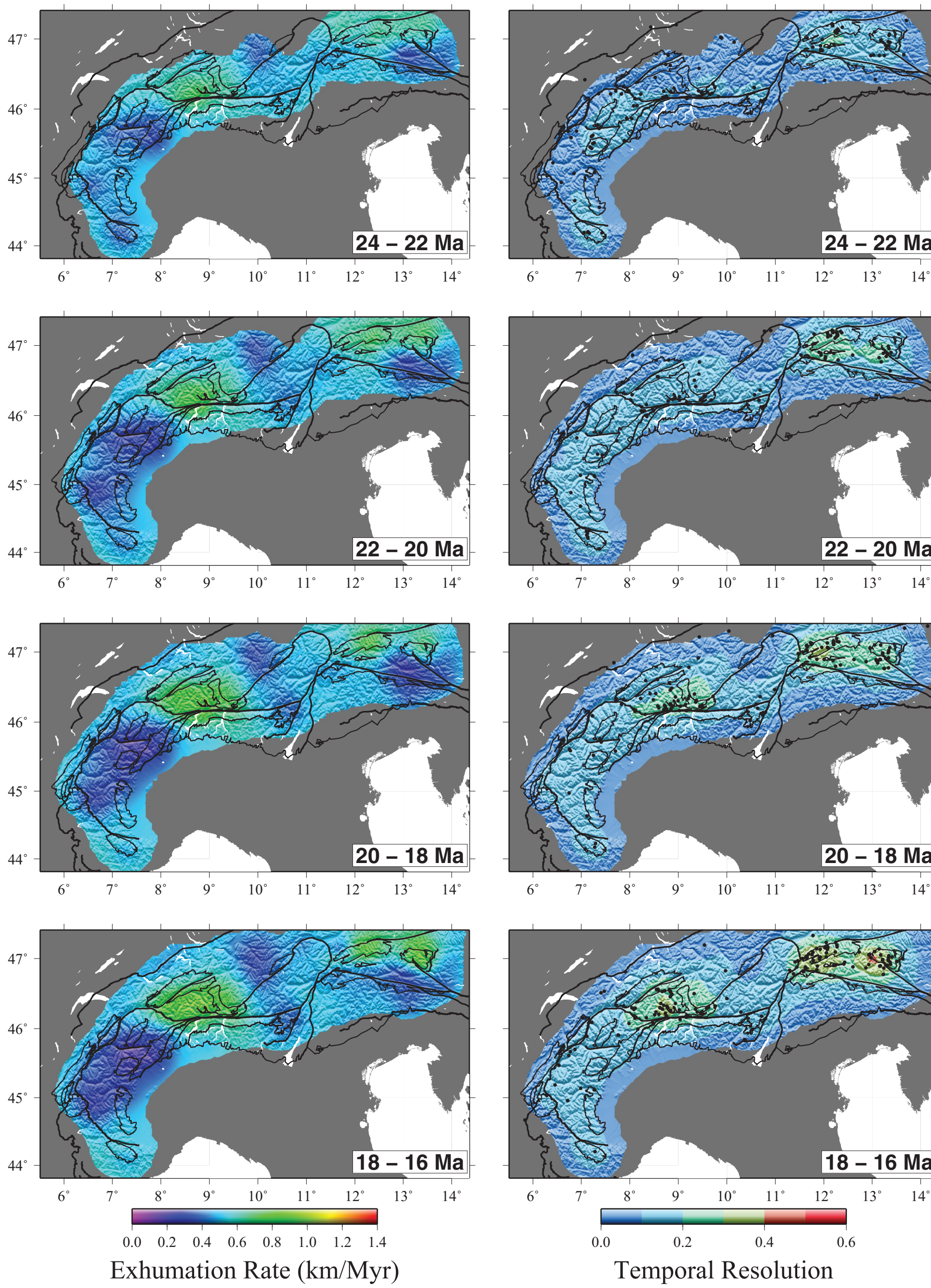

Fig. 7. Refer to figure 6 caption for details.

The various models are presented as perturbations from the preferred solution. We explore a wide range of possible models by investigating possible exhumation histories at representative locations across the Alps (see locations in fig. 1) with the aim

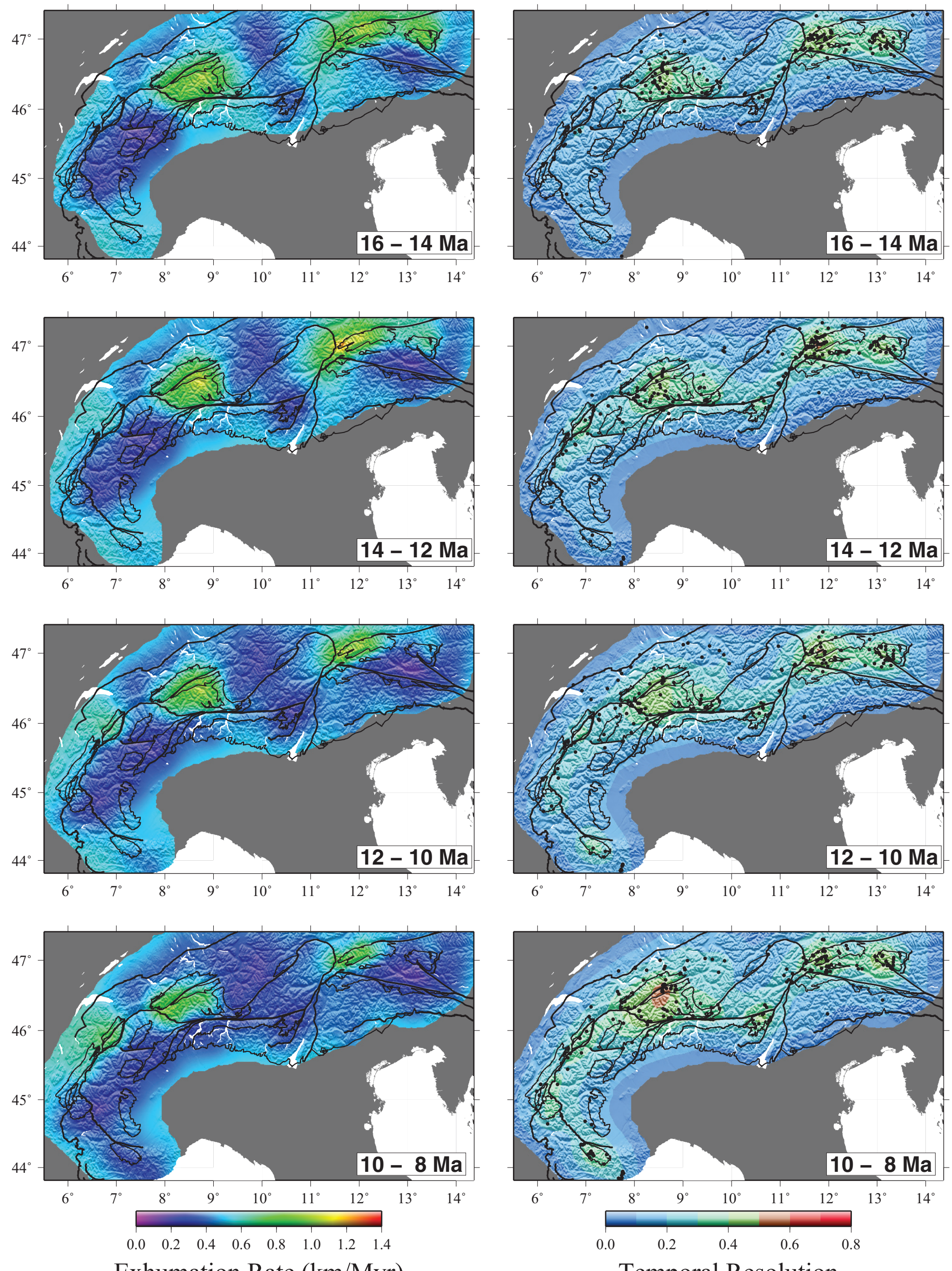

Fig. 8. Refer to figure 6 caption for details.

to determine which features of the result are robust. In the subsequent figures, each inversion result is plotted as a single exhumation rate history. Due to the correlation structure amongst model parameters, it is not possible to change model parameterization through time.

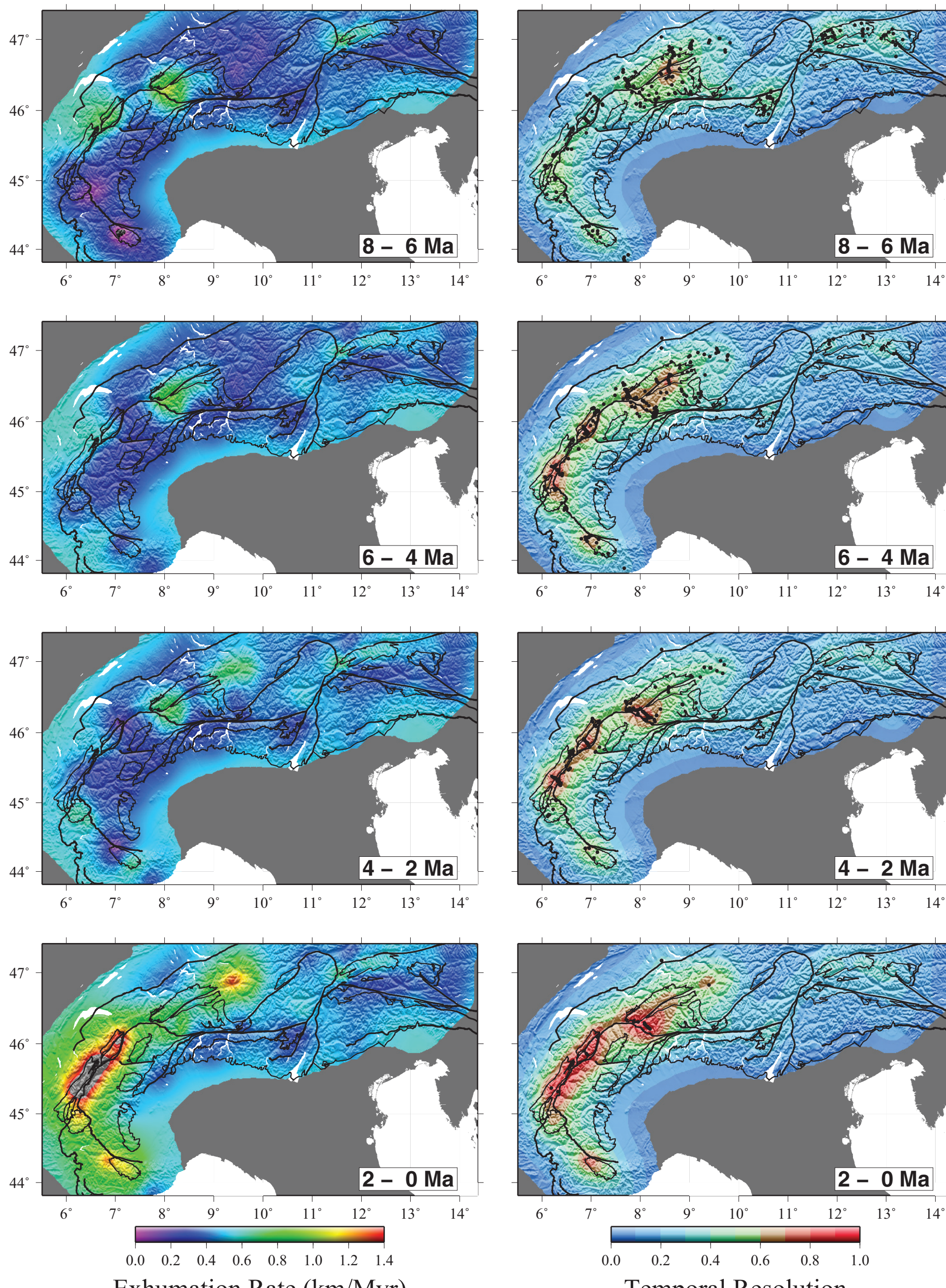

Fig. 9. Refer to figure 6 caption for details.

Note that our results are also sensitive to the *a priori* mean exhumation rate in areas and time intervals for which no data are available. Nevertheless, we found that the trends and patterns of our exhumation functions show little sensitivity to *a priori* exhumation rate if we choose values between 0.3 to 1 km/Myr.

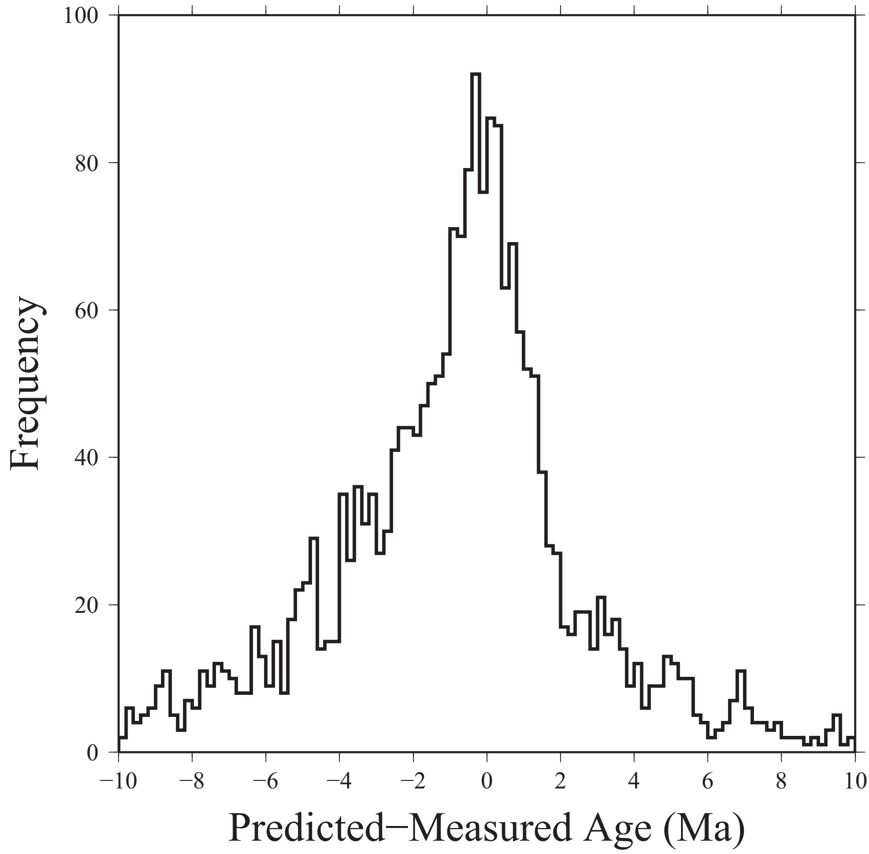

Fig. 10. The difference between the modeled and predicted ages. Note, the general shift towards negative values, that is the model predicting ages that are younger, as discussed in the text.

Argentera Massif.—The exhumation history for the Argentera Massif inferred from figure 1 is very sensitive to the time step length. All histories with time step lengths shorter than 6 Myr show rates around 0.4 km/Myr between 28 Ma and ~10 Ma and significantly faster rates (0.9 km/Myr), for the more recent history. The precise rate during this last period of fast exhumation is correlated with the timing of the onset of fast exhumation.

The sensitivity of the exhumation history to the geothermal gradient varies through time. Higher surface geothermal gradients reduce exhumation rates for the recent history. However, a recent increase of exhumation rate is still inferred for models that predict present day geothermal gradients of 45 °C/km, which is higher than the observed geothermal gradient. The earlier phase of exhumation, between 28 Ma and ~10 Ma, is sensitive to the geothermal gradient given that different systems, sensitive to different closure depths, are used to infer exhumation rate. Therefore, changes in the geothermal gradient will lead to large differences between the mean closure depths for different thermochronometric systems.

Perturbations from the *a priori* exhumation rate are accentuated by increasing the *a priori* variance, particularly during slow exhumation (25–20 Ma), at ~6 Ma and finally during final fast exhumation. This is expected as the variance acts as a damping

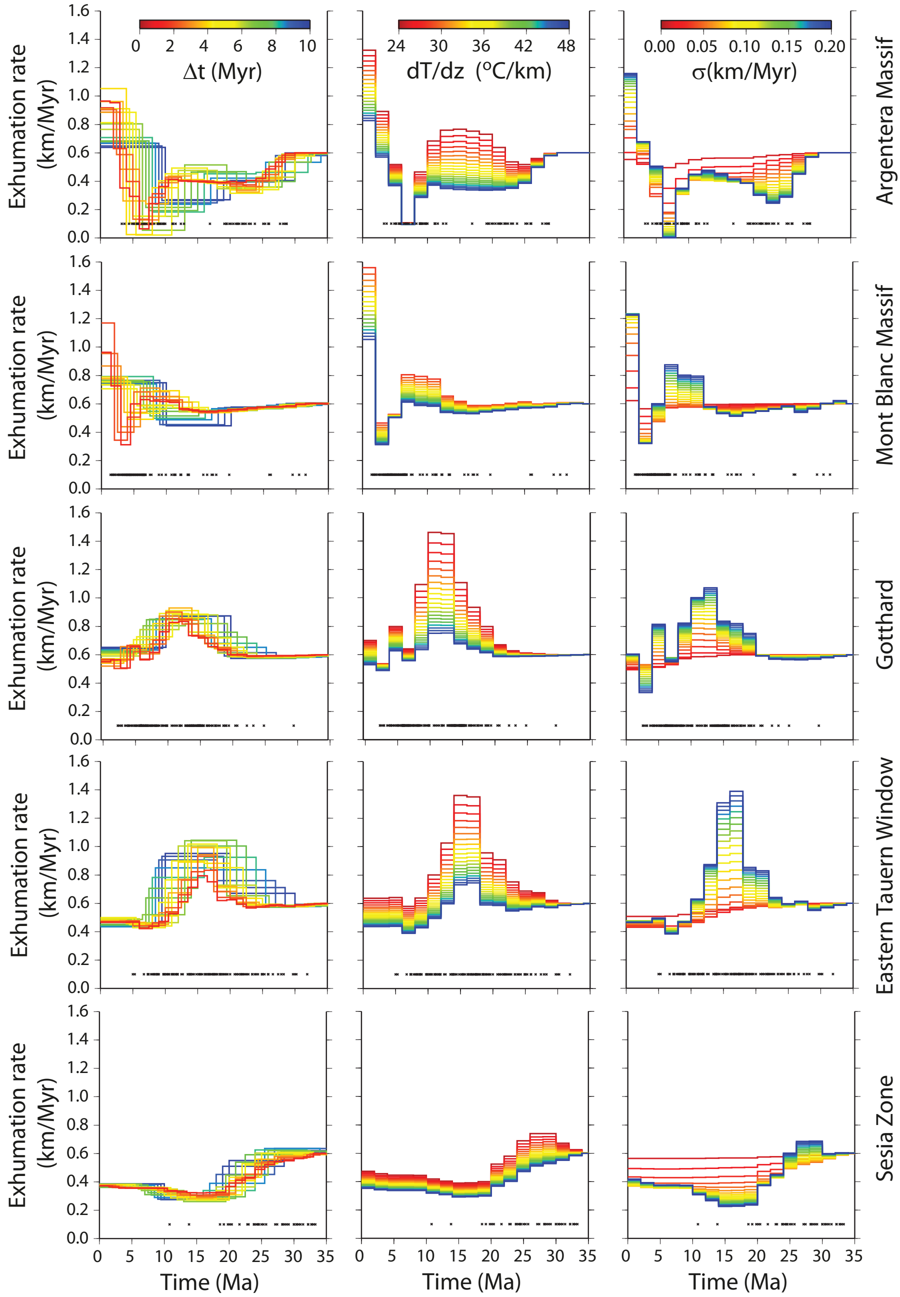

Fig. 11. Exhumation histories for the Argentera Massif, Mont Blanc, Gotthard, Eastern Tauern Window and Sesia Zone as function of inversion parameters and each row corresponds to a different location. Left panels: exhumation histories for various time step lengths; center panels: exhumation histories for various values of the final average surface geothermal gradient; right panels: exhumation histories for various values of the *a priori* standard deviation of exhumation rate. The black crosses show ages that fall within one correlation length of the control point.

parameter in the inversion scheme, dictating the degree of solution smoothness through time.

Mont Blanc Massif.—The exhumation history for the Mont Blanc Massif is similar to that of the Argentera massif. Short time steps lengths result in the appearance of periods of slow rates at 5 Ma, before the recent onset of fast exhumation. The increase of exhumation rates within the last 5 Myr in the Mont Blanc massif is observed for all models that have time step lengths shorter than 5 Myr.

Sensitivity of the inferred exhumation rate history to the thermal model is most pronounced for the most recent times. Note however, that even with a unrealistically high surface geothermal gradient of ~45 °C/km, high exhumation rates in the late history are still inferred.

The most recent stage of fast exhumation in the Mont Blanc can be suppressed by using a very low *a priori* variance in exhumation rate.

Gotthard Massif.—High rates are inferred between 10 and 15 Ma of up to 1.6 km/Myr for all time step lengths, but only for very low modern-day geothermal gradients (24 °C/km). In contrast to Argentera (fig. 9) and Mont Blanc (fig. 9), exhumation rates are low between 0 to 5 Ma regardless of the time step length. Inferred exhumation rates are most sensitive to the choice of the thermal model during the period of high exhumation rate, that is, from 10 to 15 Ma. In spite of this, all models predict a period of fast exhumation during this time interval. Inferred rates during this 10 to 15 Ma interval increase with a higher *a priori* standard deviation, as expected.

Eastern Tauern Window.—A period of fast exhumation is observed, regardless of the time step length from 10 to 20 Ma. All time step lengths indicate low recent exhumation rates. However, the period of fast exhumation becomes systematically shorter as time step length decreases, ultimately concentrating between 15 Ma and 18 Ma. As was the case in the Gotthard Massif, the interval of fast exhumation and rates of exhumation during this interval both increase with decreased surface geothermal gradients. Exhumation rates during the period of rapid exhumation increase as the *a priori* variance increases.

Sesia Zone.—The decrease in exhumation rates after 24 Ma is independent of the time step lengths we tested. Exhumation rates are sensitive to changes in the thermal model from 30 to 20 Ma, with lower geothermal gradients yielding faster rates, again due to the resolution provided by ages with different closure temperatures due to the variable thermochronometric systems used to infer exhumation rates during this particular time interval. The exhumation rates are most sensitive to the *a priori* variance during the early stages of exhumation. A higher *a priori* variance yields higher exhumation rates from 25 to 30 Ma but slower rates from 10 to 14 Ma.

DISCUSSION OF THE TECTONIC EVOLUTION OF THE ALPS IN THE CONTEXT OF INVERSION RESULTS

In the following, we discuss the inversion results obtained from the preferred model configuration presented in figure 6 to figure 9. In view of the sensitivity study presented in figure 11, we only discuss robust features of the inversion results.

Oligocene

Very few ages are available for this time and hence, temporal resolution is poor, particularly before 28 Ma (fig. 6). Moderately high rates are observed in the Sesia Zone, the Southern Alps, the area south of the Tauern Window and an area within the Austroalpine units northwest of the Adamello. These areas are located within the upper (Adria-derived) plate of the Alpine orogen. After 28 Ma (fig. 6) relatively high rates can be inferred from ages available from a wider area. The area of fast exhumation gradually spreads into the southern part of the Lepontine dome and elevated rates are also found in the Tauern Window.

The period between 35 and 24 Ma is characterized by a decrease of convergence rates due to collision between Europe and Adria, which also may have triggered slab break-off of the European Plate below the central Alps, at about 32 Ma, and the onset of retro-shearing along the Insubric Line (von Blanckenburg and Davies, 1995; Schmid and others, 1996). These processes will lead to higher rates of erosion within the upper plate and parts of the European lower plate that are adjacent to the Insubric Line (southern Lepontine dome and Bergell intrusion and Tauern Window).

Early Miocene

After 24 Ma we resolve rapid rates of exhumation across the entire Lepontine dome, and decreased rates in the Sesia Zone and adjacent areas of the Western Alps. Lower exhumation rates in the Western Alps are expected following the exhumation associated with the exposure of high-pressure rocks (Babist and others, 2006), although this rapid phase of exhumation is not investigated here. In addition, this area, unlike the Lepontine dome or the Tauern Window, was much less affected by subsequent Barrow-type metamorphism (Bousquet and others, 2008).

An area of high exhumation rate, well-resolved by the data, is the Tauern Window. Here exhumation rates peak between about 20 to 15 Ma, with rates of 0.7 km/My or more (see fig. 11). This signal is likely a response to contemporaneous orogen-parallel stretching across Brenner and Katschberg normal faults (von Blanckenburg and others, 1989; Fügenschuh and others, 1997; Luth and Willingshofer, 2008; Scharf and others, 2013; Schmid and others, 2013), triggered by the South Alpine indenter east of the Giudicarie Line (Rosenberg and others, 2007). This likely led to orogen-perpendicular shortening and rock uplift, leading to erosion.

Orogen-parallel extension also occurred at the Simplon Fault delimiting the Lepontine dome to the west during the same 20 to 15 Ma time interval, (Schlunegger and Willett, 1999; Campani and others, 2010a, 2010b). Hence, tectonic unroofing by orogen-parallel normal faulting enhanced exhumation rates in the internal parts of the lower (European) plate. As these internal units are progressively accreted to the Alpine orogen, crustal thickening occurs by pro-and retro-shearing leading to rock uplift and enhanced erosion rates (for example, Schlunegger and others, 1997; Schlunegger and Willett, 1999).

Between 20 and 16 Ma, data from the external massifs of the Western Alps begin to resolve exhumation rates of approximately 0.4 km/Myr, as indicated in previous local studies (van der Beek and others, 2010; Glotzbach and others, 2011). Note, however, that the highest exhumation rates are restricted to the Aar and Gotthard Massifs of the Central Alps, and the Lepontine Dome. During this same time interval, we infer high exhumation rates in the area of the Tauern Window. Conversely, exhumation rate continues to decrease south of the eastern Tauern Window and, very markedly, in the Sesia Zone and surrounding internal parts of the Western Alps, including the Gran Paradiso area. This is consistent with regional studies from the Internal Crystalline Massifs that show that exhumation rates were slow during the last ~20 Myr, with average rates of 0.2 km/Myr (Hurford and Hunziker, 1989; Carrapa and others, 2003; Tricart and others, 2007).

Our results are consistent with foreland propagation of thrusting in the Western and Central Alps inferred from the depositional evolution in the Alpine foreland (Kempf and others, 1999). Foreland propagation from about 32 Ma onwards caused burial and heating of the external massifs. Subsequently, from about 20 Ma onwards, these external areas started to accrete to the Alpine orogen. This is a process that probably triggered erosion-driven exhumation in the external massifs (for example, Fügenschuh and Schmid, 2003). After approximately 20 Ma, the more internal

Penninic areas, the Sesia Zone and the Austroalpine units of Switzerland and Austria north of the Periadriatic line, remained tectonically inactive, which explains the rather slow exhumation rates resolved in these areas. In the internal areas, exhumation rate is only high along the Insubric line (Beaumont and others, 1994; Schmid and others, 1996).

Middle Miocene

Exhumation rate in the Lepontine dome continues to increase and the area of high rates further propagates towards the north into the Aar and Gotthard regions between 16 to 12 Ma. This is consistent with the work of Werner (1985) on the exhumation history of this same area. A possible cause of this northwards migration of high exhumation rates after 16 Ma, is the continued northward foreland propagation. This leads to further under-plating of the European upper crust within, and underneath, the Aar and Gotthard massifs (Michalski and Soom, 1990; Schmid and others, 1996; Pfiffner and others, 2002). In addition, exhumation rates decrease across the southern Lepontine Dome and Bergell Intrusion, where exhumation rates subsequently slowed to ~0.4 km/Myr by 16 Ma and continued to slow to ~0.2 km/Myr by 5 Ma (Wagner and others, 1977; Wagner and others, 1979; Mahéo and others, 2012; Fox and others, 2014b).

It is noteworthy that we infer low exhumation rates within the external massifs of the Western Alps during the Mid-Miocene. This indicates that propagation into the European foreland occurred during a significantly later stage in the Western Alps.

Our results indicate that exhumation rate continues to increase in the western parts of the Tauern Window and remains high over the rest of the Tauern Window, consistent with recent structural studies (Scharf and others, 2013). In the eastern Tauern Window, exhumation rate decreases with respect to the previous time interval, and significantly drops in the Austroalpine units south of the Tauern Window and the adjacent Periadriatic Line. Tectonic unroofing likely played an important role in the vicinity of the Simplon normal fault (Grasemann and Mancktelow, 1993; Campani and others, 2010b) and explains the marked gradient in exhumation rate across the Simplon normal fault, resolved by the data during the 16 to 12 Ma interval. This gradient in exhumation rate is more diffuse, and not discrete, across this normal fault due to the smoothness imposed by our analysis.

Late Miocene

After 12 Ma, we observe that exhumation rates in the Aar and Gotthard Massifs continue to decrease, a trend that initiated somewhat earlier. Local studies in the eastern central Aar and adjacent Gotthard Massif have found a similar decrease in exhumation rate (Reinecker and others, 2008; Glotzbach and others, 2010) with fairly constant exhumation rates of 0.5 km/Myr since 14 Ma. In contrast, we infer that exhumation rates start to increase across the Mont Blanc and Belledonne External Crystalline Massifs of the Western Alps, and continues to increase until about 8 Ma.

Within the Lepontine dome, however, the area of fast exhumation starts to migrate westward into the area adjacent to the Simplon normal fault. In the eastern part of the Lepontine dome, the area of fast exhumation ends east at the Forcola normal fault (Meyre and others, 1998), an orogen perpendicular normal fault.

During the time interval 10 to 8 Ma, exhumation rate remains slow within the Argentera and Pelvoux massifs but increased within the Mont Blanc, Aiguille Rouge and Belledonne Massifs. Exhumation rates in the footwall of the Simplon fault begin to increase after 10 Ma and culminate during the 8 to 6 Ma time interval. Differences in exhumation rate across the Forcola normal fault are also resolved for the 10 to 6 Ma time interval. Exhumation rates within the Eastern Alps and adjacent western Tauern Window continuously decrease after 10 Ma. However, in the eastern Tauern Window, exhumation rate remains elevated to the present day, suggesting that activity of the Giudicarie line and Brenner normal fault decreased but did not completely stop.

A general trend towards slower exhumation rates is evident for the 8 to 6 Ma time interval, most notable in the Argentera and the Pelvoux External Massifs and adjacent areas (fig. 9).

Plio–Pleistocene

From 6 to 4 Ma, exhumation rate at the southern end of the Argentera Massif slowly increases to around 0.4 km/Myr while the northern half of the Argentera Massif continues to exhume slowly. Exhumation rate increases across the Belledonne between 6 to 2 Ma. Further to the north and within the External Crystalline Massifs, low exhumation rates are resolved in the Mont Blanc and Aiguilles Rouges massifs until 2 Ma, in keeping with the detailed work of Glotzbach and others (2011). Within the Mont Blanc Massif, we even see a decrease in exhumation rates after 6 Ma, particularly in its NE corner. In the western Lepontine, an area of high exhumation rate persists from 6 Ma to the present day. In addition, a region of high exhumation rate emerges after 4 Ma east of the Aar massif, namely in the Chur area, quickly accelerating thereafter, as noted previously by (Hurford and others, 1989; Persaud and Pfiffner, 2004; Reinecker and others, 2008; Vernon and others, 2008). Exhumation rates have increased slightly again across much of the Eastern Alps. These general trends are possibly related to possible changes during the Central Europe reorganization of external stress field at 6 to 5 Ma (Horváth and Cloetingh, 1996; Peresson and Decker, 1997; Sanders and others, 1999; Gerner and others, 1999); however this signal is not very well resolved. Finally, in the Eastern Alps, the southern margin of the Tauern Window continues to exhume slowly.

By 4 to 2 Ma exhumation rates across the Eastern Alps remain unchanged with respect to the previous time interval (fig. 9). Slow rates are also resolved north of the Argentera and NE of the Mont Blanc. This contrasts estimations of erosion based on sediment flux analyses (Kuhlemann and others, 2002; Kuhlemann and Kempf, 2002) that indicate an increase in exhumation rates during this time interval. The western Lepontine continued to exhume at high rates, although the rates in the rest of the Lepontine Dome have generally decreased with respect to the previous time interval.

A dramatic and abrupt change in exhumation rate is seen after 2 Ma, leading to high rates in restricted parts of the Alps (fig. 9). After the previous trend towards decreasing rates a sudden and large increase of exhumation rate is inferred across the Belledonne, Pelvoux and Mont Blanc Massifs, extending somewhat less dramatically into the area of the Argentera massif, all along the arc of the Western Alps (Fox and others, 2015). Note that this increase is relatively insignificant in the area of the Aar and Gotthard Massifs, consistent with the work of Glotzbach and others (2010). The near-circular area of high exhumation rates in the Chur region that started earlier, that is, at 4 Ma, continues to increase after 2 Ma. It is important to note that the circular nature of the Chur anomaly may be a result of the smoothness imposed. Changes after 2 Ma are very minor or absent elsewhere.

The Chur area is characterized by recent rock uplift rates in excess of 1 km/Myr as measured by geodetic methods (Schlatter and others, 2005; Brockmann and others, 2009). This is very similar to our exhumation rates in terms of magnitude and spatial pattern. This same area is known for its high present-day sediment yield due to enhanced water and ice discharge during the Pleistocene parallel to the orogen, as well for its source rocks (calcschists) with low erosional resistance (Schlunegger and Hinderer, 2001; Korup and Schlunegger, 2009). Moreover, the area is characterized by a high density of earthquake epicenters (Deichmann, 1992) possibly representing the physical response of the orogen to perturbations of stress caused by surface erosion. According to Kühni and Pfiffner (2001) the capture of ancestral orogen-perpendicular rivers by longitudinal rivers such as the Rhine river near Chur took place after mid-Miocene times and coeval with the final phase of the Aar massif uplift. Furthermore, drainage reorganization and capture of ancestral rivers alone would not lead to a change in erosion rate that is sufficient to explain the Chur anomaly (Yanites and others, 2013).

The recent increase in exhumation rates (post 2 Ma, according to our inversion results) in the external massifs of the Western Alps reaches values exceeding 1.5 km/Myr and represents the strongest signal within the investigated area. In general, the exhumation history we infer for the external arc of the Western Alps is consistent with previous local studies. Several studies on the exhumation history of the External Crystalline Massifs of the Western Alps (Argentera: Bigot-Cormier and others, 2006; Pelvoux: van der Beek and others, 2010; Mont Blanc: Leloup and others, 2005 and Glotzbach and others, 2008), indicate a three stage evolution: First, exhumation rates peaked at around 6 to 7 Ma, dropped by an order of magnitude later on, only to finally increase again during the Plio-Quaternary to values around 0.5 to 1 km/Myr. Egli and Mancktelow (2013) showed that none of the major faults or shear zones directly bounding the Mont Blanc massif were actively accommodating vertical motion in Late Neogene times and that young exhumation is therefore not controlled by these structures. This most recent and final increase in exhumation rate has been explained by recent valley carving in response to glacial erosion (Leloup and others, 2005; Glotzbach and others, 2008; Valla and others, 2011). Importantly, removing ages obtained from samples from valley bottoms from our analysis does not remove this signal (Fox and others, 2015). Furthermore, if glacial erosion alone is indeed responsible for the recent increase in exhumation rates the question arises why it is only the external Arc of the Western Alps that is affected and not the equally glaciated Central and Eastern Alps (Sternai and others, 2011)?

It is well known that the Central Alps have a large crustal root compared with the topographic load and in relation to a their positive Bouguer gravity anomaly (Lyon-Caen and Molnar, 1989; Kissling, 1993). As pointed out by Kissling (2008), this is related to the slab weight of the subducted oceanic lithosphere of Alpine Tethys basins that forces the European lithosphere, and thereby also the European Moho, to reach a greater depth than is expected if the crust were in isostatic equilibrium. As a result of the very recent slab break-off event in the Western Alps (Lippitsch and others, 2003) (fig. 2) slab weight unloading by delamination along the Moho Kissling (2008) can cause sudden rock uplift.

However, in order for the change in rock uplift to result in an immediate change in exhumation rate, erosion rates are also required to change abruptly. In a fluvial erosive environment, an increase in rock uplift rate due to slab detachment would lead to an increase in the topographic gradient. In turn, this leads to higher erosive potential of rivers and, therefore, increased erosion rates and higher fluvial relief (for example, Howard and Kerby, 1983; Whipple and Tucker, 1999; Snyder and others, 2000). This fluvial erosion mechanism seems unlikely for as the fluvial relief across the Alps is relatively uniform (Sternai and others, 2012). This uniformity suggests that prior to the onset of rapid exhumation, the topography of the Western Alps would have been very subdued with respect to the Central and Eastern Alps, and there is no evidence for such subdued topography (Sternai and others, 2012).

When glaciers are the dominant erosive agents, the response to enhanced rock uplift is very different. Most glacial erosion models assume erosion rate to be proportional to ice sliding velocity raised to some power (Harbor and others, 1988) and periglacial processes such as frost cracking can reduce high peaks to rock debris easily transported away by glaciers (Hales and Roering, 2009; Delunel and others, 2010). These two processes imply that glacial erosion is most efficient at and above the

Equilibrium Line Altitude (ELA), that separates the ice accumulation and ablation regions of a glacier (Anderson and others, 2006; Egholm and others, 2009; Sternai and others, 2013), at least outside of the high latitudes (Thomson and others, 2010). If glacial and periglacial erosion is highly efficient above the ELA, once the mountains in the frontal Western Alpine arc reached a height with significant area above the ELA, for example, due to slab detachment, the erosion rate is expected to increase.

In summary, detachment of the slab removes a vertical load beneath the Western Alps, which would drive surface uplift. Numerical models of slab detachment predict that the resulting rock uplift rate could be as high as 0.8 km/Myr across wavelengths of up to 100 km (Duretz and others, 2010). Other data also support tectonic surface uplift consistent with active slab detachment below the Western Alps: Earthquake focal mechanisms (Delacou and others, 2004), GPS geodesy (D'Agostino and others, 2008), structural analysis (Sue and others, 2007), and tilting of the surrounding foreland (Champagnac and others, 2008), crustal seismicity across the northern foreland Singer and others (2014) all suggest that the Western Alps are presently undergoing horizontal extension, crustal thinning and surface uplift (Sue and others, 2007). This ongoing process, local to the Western Alps, provides a mechanism to explain the very high exhumation rates in the Western Alps (Fox and others, 2015).

SUMMARY AND CONCLUSIONS

We have applied a linear inversion procedure to extract an exhumation function, variable in both space and time, from over 2500 thermochronometric ages across the Alps. Through a series of sensitivity tests, we have highlighted typical variations in the inferred exhumation rates due to changes in the model configuration. The sensitivity tests also provide an insight into which features of the results are robust across the range of model configurations. Key results from our analysis include:

- Exhumation rates are initially fast in the internal arc of the Western Alps at rates up to ~0.8 km/Myr at 30 Ma, and then decreasing at ~20 Ma to 0.3 km/Myr, and remaining low to the present.
- At the same time as exhumation rate decreases across the internal units, exhumation rates across the ECMs of Western Alps increase to rates of 0.6 km/Myr.
- The onset of high exhumation rates within the Tauern Window and the Lepontine Dome occurs at a similar time, that is at around 20 Ma ago.
- The diachronous unroofing of Eastern (~18 Ma) and Western (~15 Ma) Tauern window is possibly the result of the indentation of the Southalpine units east of the Giudicarie Belt at ~20 Ma.
- Exhumation rates in the Chur area begin to increase at ~4 Ma and are locally high within the last 2 Myr. They are possibly caused by a change in the configuration of the Alpine drainage network.
- Our study does not confirm an overall increase in exhumation rates at around 5 Ma over the entire orogen; instead a more recent increase at 2 Ma is inferred.
- We find that the Western Alps exhibit a 2 to 3 fold increase in exhumation rate over the last 2 Ma during a recent event not seen in the Eastern Alps, in spite of very similar topographic characteristics. We interpret this as the result of rock uplift in response to detachment of the European slab in the Western Alps (Lippitsch and others, 2003), combined with efficient glacial erosion (for example, Egholm and others, 2009; Sternai and others, 2013).
- The limited region of high exhumation rate in the Western Alps corresponds to a region where the seismic p-wave velocity anomaly in the upper mantle has been interpreted as indicating recent detachment of the European mantle slab (Lippitsch and others, 2003), figure 3. Further support for this tectonic

scenario comes from observations indicating crustal extension (Sue and others, 1999; Delacou and others, 2004; Selverstone, 2005; Champagnac and others, 2006).

By increasing the number of timesteps (decreasing Δt) we are able to better approximate the timings of changes in exhumation rate. However, the number of ages within each time interval is naturally reduced by doing so, and hence, shorter time intervals are more sensitive to the *a priori* model and to noise in the data. In turn, this causes spurious oscillations and poor resolution.

At present the distribution of thermochronometric ages across the Alps is unparalleled by any other mountain belt; nevertheless there are geographical regions that remain poorly resolved. In general poor resolution relates to two factors; 1) the suitability of different lithologies for thermochronometric analysis results in large geographical regions with no age control; 2) very slowly exhuming regions where the thermochronometric ages are older than 35 Ma. Across these regions of old ages, the average exhumation rate has to be slow since 35 Ma. However, recent erosion rates may have increased without exposing reset ages. In order to increase the resolution in these slowly eroding regions, younger ages should be acquired. This would be possible through obtaining ages with thermochronometric systems sensitive to lower closure temperatures.

ACKNOWLEDGMENTS

We would like to thank the TopoEurope and ThermoEurope team for invaluable contributions at all stages of the project. In particular we would like to thank Jean Braun, Peter van der Beek and Pete Reiners for formal reviews. We also thank Mark Brandon, Ladsi Rybach, Jean–Daniel Champagnac, Piere Valla and Edi Kissling for helpful comments and suggestions. We thank Stefan Luth, Andreas Woffler, Audrey Bertrand, Neil Manktelow and Antoine Vernon for kindly making compiled datasets available to us. The Brutus high performance computer facilities of the ETHZ were used to perform all calculations and figures were produced using GMT (Wessel and Smith, 1998).

APPENDIX

Ages have been complied from the following sources: Bistacchi and others (2001); Bürgi and Klötzli (1990); Carpéna (1992); Ciancaleoni (ms, 2005); Coyle (ms, 1994); Dunkl and others (2003); Elias (1998); Flisch (1986); Fügenschuh and Schmid (2003); Fügenschuh (ms, 1995); Fügenschuh and others (1999); Giger (ms, 1991); Grundmann and Morteani (1985); Hunziker and others (1992); Hurford and Hunziker (1989); Hurford and others (1991); Hurford (1986); Knaus (ms, 1990); Lelarge (ms, 1993); Leloup and others (2005); Lihou and others (1995); Malusà and others (2005); Martin and others (1998); Michalski and Soom (1990); Most (ms, 2003); Rahn and others (1997); Soom (ms, 1990); Sabil (ms, 1994); Schaer and others (1975); Schwartz (ms, 2000); Seward and Mancktelow (1994); Seward and others (1999); Staufenberg (1987); Steenken and others (2002); Steiner (1984); Timar-Geng and others (2004); Trautwein (ms, 2000); Tricart and others (2007); Viola (ms, 2000); Viola and others (2001, 2003); Wagner and Reimer (1972); Wagner and others (1977); Wagner and others (1979); Weh (ms, 1998); Bigot-Cormier (ms, 2002); Brügel and others (2003); Hejl and Grundmann (1989); Hejl (1997); Zattin and others (2003); Keller and others (2005); Zattin and others (2006); Hurford and Hunziker (1985); Spiegel and others (2000); Stockhert and others (1999); Dunkl and Demény (1997); Glotzbach and others (2010, 2008); Pignalosa and others (2011); Foeken and others (2003); Wölfler and others (2008); Sanchez and others (2011); Reverman and others (2012); Glotzbach and others (2008, 2009, 2010, 2011); Mahéo and others (2012); Fox and others (2014b); van der Beek and others (2010); Foeken and others (2007); Valla and others (2011); Valla and others (2012); Reinecker and others (2008); Cederbom and others (2004, 2011); Allaz (ms, 2008); Markley and others (1998); Hetherington and Villa (2007); Romer and others (1996); Hunziker (1970); Purdy and Jäger (1976); Hurford (1986); Bürgi and Klötzli (1990); Ferrara and others (1962); Jäger and Faul (1959); Armstrong and others (1966); Hunziker and Bearth (1969).

REFERENCES

Allaz, J., ms, 2008, Metamorphic Evolution in the Northern Central Alps: Linking ^{39}Ar–^{40}Ar Dating with Thermobarometry: Bern, Switzerland, University of Bern, Ph. D. thesis, 208 p.

Allen, P. A., Crampton, S. L., and Sinclair, H. D., 1991, The inception and early evolution of the North Alpine Foreland Basin, Switzerland: Basin Research, v. 3, n. 3, p. 143–163, http://dx.doi.org/10.1111/j.1365-2117.1991.tb00124.x

Anderson, R. S., Molnar, P., and Kessler, M. A., 2006, Features of glacial valley profiles simply explained: Journal of Geophysical Research-Earth Surface, v. 111, n. F1, F01004, http://dx.doi.org/10.1029/2005JF000344

Argand, E., 1911, Les nappes de recouvrement des Alpes occidentales et les territoires environnants: Matériaux Carte Géologicae Suisse, v. 27.

——— 1916, Sur l'arc des Alpes occidentales: Eclogae Geologicae Helvetiae, v. 14, p. 145–191.

Armstrong, R. L., Jäger, E., and Eberhardt, P., 1966, A comparison of K-Ar and Rb-Sr ages on Alpine biotites: Earth and Planetary Science Letters, v. 1, n. 1, p. 13–19, http://dx.doi.org/10.1016/0012-821X(66)90097-5

Babist, J., Handy, M. R., Konrad-Schmolke, M., and Hammerschmidt, K., 2006, Precollisional, multistage exhumation of subducted continental crust: The Sesia Zone, western Alps: Tectonics, v. 25, n. 6, TC6008, http://dx.doi.org/10.1029/2005TC001927

Beaumont, C., Fullsack, P., and Hamilton, J., 1994, Styles of crustal deformation in compressional orogens caused by subduction of the underlying lithosphere: Tectonophysics, v. 232, n. 1–4, p. 119–132, http://dx.doi.org/10.1016/0040-1951(94)90079-5

Beaumont, C., Ellis, S., Hamilton, J., and Fullsack, P., 1996, Mechanical model for subduction-collision tectonics of Alpine-type compressional orogens: Geology, v. 24, n. 8, p. 675–678, http://dx.doi.org/10.1130/0091-7613(1996)024<0675:MMFSCT>2.3.CO;2

Bernet, M., Zattin, M., Garver, J. I., Brandon, M. T., and Vance, J. A., 2001, Steady-state exhumation of the European Alps: Geology, 29, n. 1, p. 35–39, http://dx.doi.org/10.1130/0091-7613(2001)029<0035:SSEOTE>2.0.CO;2

Bernet, M., Brandon, M. T., Garver, J. I., and Molitor, B. R., 2004, Fundamentals of detrital zircon fission-track analysis for provenance and exhumation studies with examples from the European Alps, *in* Bernet, M., and Spiegel, C., editors, Detrital thermochronology-Provenance Analysis, Exhumation and Landscape Evolution of Mountain Belts: Geological Society of America Special Papers, v. 378, p. 25–36, http://dx.doi.org/10.1130/0-8137-2378-7.25

Bernet, M., Brandon, M., Garver, J., Balestieri, M. L., Ventura, B., and Zattin, M., 2009, Exhuming the Alps through time: Clues from detrital zircon fission-track thermochronology: Basin Research, v. 21, n. 6, p. 781–798, http://dx.doi.org/10.1111/j.1365-2117.2009.00400.x

Bigot-Cormier, F., ms, 2002, La surrection du massif cristallin externe de l'Argentera (France–Italie) et ses relations avec la déformation pliocène de la marge Nord-Ligure: Arguments thermochronologiques (traces de fission), géomorphologiques et interprétations de sismique marine: Nice, France, University of Nice, Ph. D. thesis, 352 p.

Bigot-Cormier, F., Sosson, M., Poupeau, G., Stéphan, J. F., and Labrin, E., 2006, The denudation history of the Argentera Alpine External Crystalline Massif (Western Alps, France-Italy): An overview from the analysis of fission tracks in apatites and zircons: Geodinamica Acta, v. 19, n. 6, p. 455–473, http://dx.doi.org/10.3166/ga.19.455-473

Bistacchi, A., Dal Piaz, G., Massironi, M., Zattin, M., and Balestrieri, M., 2001, The Aosta-Ranzola extensional fault system and Oligocene-Present evolution of the Austroalpine-Penninic wedge in the northwestern Alps: International Journal of Earth Sciences, v. 90, n. 3, p. 654–667, http://dx.doi.org/10.1007/s005310000178

Bodmer, H. P., and Rybach, L., 1984, Geothermal map of Switzerland: Heat flow density: Contributions to the Geology of Switzerland, Geophysics Series, 22.

Boschi, L., Faccenna, C., and Becker, T. W., 2010, Mantle structure and dynamic topography in the Mediterranean Basin: Geophysical Research Letters, v. 37, n. 20, http://dx.doi.org/10.1029/2010GL045001

Bousquet, R., Oberhänsli, R., Goffé, B., Wiederkehr, M., Koller, F., Schmid, S. M., Schuster, R., Engi, M., Berger, A., and Martinotti, G., 2008, Metamorphism of metasediments at the scale of an orogen: A key to the Tertiary geodynamic evolution of the Alps, *in* Siegesmund, S., Fügenschuh, and Froitzheim, N., editors, Tectonic Aspects of the Alpine-Dinaride-Carpathian System: Geological Society, London, Special Publications, v. 298, p. 393–411, http://dx.doi.org/10.1144/SP298.18

Brandon, M. T., Roden-Tice, M. K., and Garver, J. I., 1998, Late Cenozoic exhumation of the Cascadia accretionary wedge in the Olympic Mountains, northwest Washington State: Geological Society of America Bulletin, v. 110, n. 8, p. 985–1009, http://dx.doi.org/10.1130/0016-7606(1998)110<0985:LCEOTC>2.3.CO;2

Brockmann, E., Ineichen, D., Marti, U., Schaer, S., Schlatter, A., and Villiger, A., 2009, Determination of Tectonic Movements in the Swiss Alps using GNSS and Levelling, *in* Kenyon, S., Pacino, M. C., and Marti, U., editors, Geodesy for Planet Earth: Berlin, Springer-Verlag Proceedings of the International Association of Geodesy Symposia 136, Buenos Aires, Argentina, August 31- September 4, 2009, p. 689–695, http://dx.doi.org/10.1007/978-3-642-20338-1_85

Brouwer, F. M., van de Zedde, D. M. A., Wortel, M. J. R., and Vissers, R. L. M., 2004, Late-orogenic heating during exhumation: Alpine PTt trajectories and thermomechanical models: Earth and Planetary Science Letters, v. 220, n. 1–2, 185–199, http://dx.doi.org/10.1016/S0012-821X(04)00050-0

Brügel, A., Dunkl, I., Frisch, W., Kuhlemann, J., and Balogh, K., 2003, Geochemistry and geochronology of gneiss pebbles from foreland molasse conglomerates: Geodynamic and paleogeographic implications

for the Oligo-Miocene evolution of the Eastern Alps: The Journal of Geology, v. 111, n. 5, p. 543–563, http://dx.doi.org/10.1086/376765
Bürgi, A., and Klötzli, U., 1990, New data on the evolutionary history of the Ivrea Zone (Northern Italy): Bulletin der Vereinigung Schweizerischer Petroleum-Geologen und-Ingenieure, v. 56, n. 130, 49–70.
Burkhard, M., 1990, Aspects of the large-scale Miocene deformation in the most external part of the Swiss Alps (Subalpine Molasse to Jura fold belt): Eclogae geologicae Helvetiae, v. 83, n. 3, 559–583.
Burkhard, M., and Sommaruga, A., 1998, Evolution of the western Swiss Molasse basin: Structural relations with the Alps and the Jura belt, *in* Mascale, A., Puigedfàbregas, Luterbacher, H. P., and Fernàndez, M., editors, Cenozoic Foreland Basins of Western Europe: Geological Society, London, Special Publications, v. 134, p. 279–298, http://dx.doi.org/10.1144/gsl.sp.1998.134.01.13
Calais, E., Nocquet, J. M., Jouanne, F., and Tardy, M., 2002, Current strain regime in the Western Alps from continuous Global Positioning System measurements, 1996-2001: Geology, v. 30, n. 7, p. 651–655, http://dx.doi.org/10.1130/0091-7613(2002)030<0651:CSRITW>2.0.CO;2
Campani, M., Herman, F., and Mancktelow, N., 2010a, Two-and three-dimensional thermal modeling of a low-angle detachment: Exhumation history of the Simplon Fault Zone, central Alps: Journal of Geophysical Research-Solid Earth, v. 115, n. B10, B10420, http://dx.doi.org/10.1029/2009JB007036
Campani, M., Mancktelow, N., Seward, D., Rolland, Y., Müller, W., and Guerra, I., 2010b, Geochronological evidence for continuous exhumation through the ductile-brittle transition along a crustal-scale low-angle normal fault: Simplon Fault Zone, central Alps: Tectonics, v. 29, n. 3, TC3002, http://dx.doi.org/10.1029/2009TC002582
Carpéna, J., 1992, Fission track dating of zircon: Zircons from Mont Blanc granite (French-Italian Alps): The Journal of Geology, v. 100, n. 4, p. 411–421, http://dx.doi.org/10.1086/629595
Carrapa, B., Wijbrans, J., and Bertotti, G., 2003, Episodic exhumation in the Western Alps: Geology, v. 31, n. 7, p. 601–605, http://dx.doi.org/10.1130/0091-7613(2003)031<0601:EEITWA>2.0.CO;2
Cederbom, C. E., Sinclair, H. D., Schlunegger, F., and Rahn, M. K., 2004, Climate-induced rebound and exhumation of the European Alps: Geology, v. 32, n. 8, 709–713, http://dx.doi.org/10.1130/G20491.1
Cederbom, C. E., van der Beek, P., Schlunegger, F., Sinclair, H. D., and Oncken, O., 2011, Rapid extensive erosion of the North Alpine foreland basin at 5–4 Ma: Basin Research, v. 23, n. 5, p. 528–550, http://dx.doi.org/10.1111/j.1365-2117.2011.00501.x
Cermak, V., 1993, Lithospheric thermal regimes in Europe: Physics of the Earth and Planetary Interiors, v. 79, n. 1–2, p. 179–193, http://dx.doi.org/10.1016/0031-9201(93)90147-2
Champagnac, J. D., Sue, C., Delacou, B., Tricart, P., Allanic, C., and Burkhard, M., 2006, Miocene lateral extrusion in the inner Western Alps revealed by dynamical fault analysis: Tectonics, v. 25, n. 3, TC3014, http://dx.doi.org/10.1029/2004TC001779
Champagnac, J. D., Molnar, P., Anderson, R. S., Sue, C., and Delacou, B., 2007, Quaternary erosion-induced isostatic rebound in the Western Alps: Geology, v. 35, n. 3, p. 195–198, http://dx.doi.org/10.1130/G23053A.1
Champagnac, J. D., van Der Beek, P., Diraison, G., and Dauphin, S., 2008, Flexural isostatic response of the Alps to increased Quaternary erosion recorded by foreland basin remnants, SE France: Terra Nova, v. 20, n. 3, p. 213–220, http://dx.doi.org/10.1111/j.1365-3121.2008.00809.x
Champagnac, J. D., Schlunegger, F., Norton, K., von Blanckenburg, F., Abbühl, L. M., and Schwab, M., 2009, Erosion-driven uplift of the modern Central Alps: Tectonophysics, v. 474, n. 1–2, p. 236–249, http://dx.doi.org/10.1016/j.tecto.2009.02.024
Ciancaleoni, L., ms, 2005, Deformation processes during the last stages of the continental collision: the brittle-ductile fault systems in the Bergell and Insubric areas (Eastern Central Alps, Switzerland – Italy): Neuchatel , Switzerland, Université de Neuchatel, Ph. D. thesis, 192 p.
Clark, S. P., Jr., and Jäger, E., 1969, Denudation rate in the Alps from geochronologic and heat flow data: American Journal of Science, v. 267, n. 10, p. 1143–1160, http://dx.doi.org/10.2475/ajs.267.10.1143
Clark, S. P., Jr., and Niblett, E. R., 1956. Terrestrial heat flow in the Swiss Alps: Geophysical Journal International, v. 7, n. 4, p. 176–195, http://dx.doi.org/10.1111/j.1365-246X.1956.tb05563.x
Coyle, D. A., ms, 1994, The application of apatite fission track analysis to problem in tectonics: Melbourne, Victoria, Australia, La Trobe University, Australia, Ph. D. thesis,
D'Agostino, N., Avallone, A., Cheloni, D., D'Anastasio, E., Mantenuto, S., and Selvaggi, G., 2008, Active tectonics of the Adriatic region from GPS and earthquake slip vectors: Journal of Geophysical Research-Solid Earth, v. 113, n. B12, p. 2156–2202, http://dx.doi.org/10.1029/2008JB005860
Dal Piaz, G., Cortiana, G., Del Moro, A., Martin, S., Pennacchioni, G., and Tartarotti, P., 2001, Tertiary age and paleostructural inferences of the eclogitic imprint in the Austroalpine outliers and Zermatt-Saas ophiolite, Western Alps: International Journal of Earth Sciences, v. 90, n. 3, p. 668–684, http://dx.doi.org/10.1007/s005310000177
Dal Piaz, G. V., Del Moro, A., Martin, S., and Venturelli, G., 1988, Post-collisional magmatism in the Ortler-Cevedale massif (Northern Italy): Jahrbuch der Geologischen Bundesanstalt, v. 131, n. 4, p. 533–551.
Deichmann, N., 1992, Structural and rheological implications of lower-crustal earthquakes below northern Switzerland: Physics of the Earth and Planetary Interiors, v. 69, n. 3–4, p. 270–280, http://dx.doi.org/10.1016/0031-9201(92)90146-M
Delacou, B., Sue, C., Champagnac, J. D., and Burkhard, M., 2004, Present-day geodynamics in the bend of the western and central Alps as constrained by earthquake analysis: Geophysical Journal International, v. 158, n. 2, p. 753–774, http://dx.doi.org/10.1111/j.1365-246X.2004.02320.x
Delunel, R., Van Der Beek, P. A., Carcaillet, J., Bourlès, D. L., and Valla, P. G., 2010, Frost-cracking control on catchment denudation rates: Insights from *in situ* produced ^{10}Be concentrations in stream sediments (Ecrins-Pelvoux massif, French Western Alps): Earth and Planetary Science Letters, v. 293, n. 1–2, p. 72–83, http://dx.doi.org/10.1016/j.epsl.2010.02.020

Diehl, T., Husen, S., Kissling, E., and Deichmann, N., 2009, High-resolution 3-D *P*-wave model of the Alpine crust: Geophysical Journal International, v. 179, n. 2, p. 1133–1147, http://dx.doi.org/10.1111/j.1365-246X.2009.04331.x
Dodson, M. H., 1973, Closure temperature in cooling geochronological and petrological systems: Contributions to Mineralogy and Petrology, v. 40, n. 3, p. 259–274, http://dx.doi.org/10.1007/BF00373790
Dunkl, I., and Demény, A., 1997, Exhumation of the Rechnitz Window at the border of the Eastern Alps and Pannonian Basin during Neogene extension: Tectonophysics, v. 272, n. 2–4, p. 197–211, p. http://dx.doi.org/10.1016/S0040-1951(96)00258-2
Dunkl, I., Frisch, W., and Grundmann, G., 2003, Zircon fission track thermochronology of the southeastern part of the Tauern Window and the adjacent Austroalpine margin, Eastern Alps: Eclogae Geologicae Helvetiae, v. 96, n. 2, p. 209–218, http://dx.doi.org/10.1007/s00015-003-1092-3
Duretz, T., Gerya, T. V., and May, D. A., 2010, Numerical modelling of spontaneous slab breakoff and subsequent topographic response: Tectonophysics, v. 502, n. 1–2, p. 244–256, http://dx.doi.org/10.1016/j.tecto.2010.05.024
Egholm, D. L., Nielsen, S. B., Pedersen, V. K., and Lesemann, J. E., 2009, Glacial effects limiting mountain height: Nature, v. 460, n. 7257, p. 884–887, http://dx.doi.org/10.1038/nature08263
Egli, D., and Mancktelow, N., 2013, The structural history of the mont blanc massif with regard to models for its recent exhumation: Swiss Journal of Geosciences, v. 106, n. 3, p. 469–489, http://dx.doi.org/10.1007/s00015-013-0153-5
Elias, J., 1998, The thermal history of the Ötztal-Stubai complex (Tyrol, Austria/Italy) in the light of the lateral extrusion model: Tübinger Geowissenschaftliche Arbeiten, Reihe A, 36, 172 p.
England, P., and Molnar, P., 1990, Surface uplift, uplift of rocks, and exhumation of rocks: Geology, v. 18, n. 12, p. 1173–1177, http://dx.doi.org/10.1130/0091-7613(1990)018<1173:SUUORA>2.3.CO;2
Escher, A., and Beaumont, C., 1997, Formation, burial and exhumation of basement nappes at crustal scale: A geometric model based on the Western Swiss-Italian Alps: Journal of Structural Geology, v. 19, n. 7, p. 955–974, http://dx.doi.org/10.1016/S0191-8141(97)00022-9
Escher, A., Hunziker, J. C., Marthaler, M., Masson, H., Sartori, M., and Steck, A., 1997, Geologic framework and structural evolution of the western Swiss-Italian Alps, *in* Pfiffner, O. A., Lehner, P., Heitzmann, P., Mueller, S., and Steck, A., editors, Deep structure of the Swiss Alps- Results of NRP: Basel, Switzerland, Birkhuauser, p. 205–221.
Faccenna, C., and Becker, T. W., 2010, Shaping mobile belts by small-scale convection: Nature, v. 465, (7298), p. 602–605, http://dx.doi.org/10.1038/nature09064
Fantoni, R., Bersezio, R., and Forcella, F., 2004, Alpine structure and deformation chronology at the southern Alps-Po Plain border in Lombardy: Bollettino della Società Geologica Italiana, v. 123, n. 3, 463–476.
Farley, K. A., 2000, Helium diffusion from apatite: General behavior as illustrated by Durango fluorapatite: Journal of Geophysical Research-Solid Earth, v. 105, n. B 2, p. 2903–2914, http://dx.doi.org/10.1029/1999JB900348
Ferrara, G., Hirt, B., Jäger, E., and Niggli, E., 1962, Rb-Sr and U-Pb age determinations on the pegmatite of I Mondei (Penninic Camughera-Moncucco-Complex, Italian Alps and some gneisses from the neighborhood): Eclogae Geologicae Helvetiae, v. 55, n. 2, p. 443–450.
Flisch, M., 1986, Die Hebungsgeschichte der oberostalpinen Silvretta-Decke seit der mittleren Kreide: Bulletin der Vereinigung schweizerische Petroleum-Geologen Ingenieure, v. 53, n. 123, p. 23–49.
Foeken, J. P. T., Dunai, T. J., Bertotti, G., and Andriessen, P. A. M., 2003, Late Miocene to present exhumation in the Ligurian Alps (southwest Alps) with evidence for accelerated denudation during the Messinian salinity crisis: Geology, v. 31, n. 9, p. 797–801, http://dx.doi.org/10.1130/G19572.1
Foeken, J. P. T., Persano, C., Stuart, F. M., and ter Voorde, M., 2007, Role of topography in isotherm perturbation: Apatite (U-Th)/He and fission track results from the Malta tunnel, Tauern Window, Austria: Tectonics, v. 26, n. 3, C3006, http://dx.doi.org/10.1029/2006TC002049
Fox, M., Herman, F., Willett, S. D., and May, D. A., 2014a, A linear inversion method to infer exhumation rates in space and time from thermochronometric data: Earth Surface Dynamics, v. 2, n. 1, p. 47–65, http://dx.doi.org/10.5194/esurf-2-47-2014
Fox, M., Reverman, R., Herman, F., Fellin, M. G., Sternai, P., and Willett, S. D., 2014b, Rock uplift and erosion rate history of the Bergell intrusion from the inversion of low temperature thermochronometric data: Geochemistry, Geophysics, Geosystems, v. 15, n. 4, p. 1235–1257, http://dx.doi.org/10.1002/2013GC005224
Fox, M., Herman, F., Kissling, E., and Willett, S. D., 2015, Rapid exhumation in the Western Alps driven by slab detachment and glacial erosion: Geology, v. 43, n. 5, p. 379–382, http://dx.doi.org/10.1130/G36411.1
Fügenschuh, B., ms, 1995, Thermal and kinematic history of the Brenner area (Eastern Alps, Tyrol): Zurich Switzerland, ETHZ, Ph. D thesis, 146 p.
Fügenschuh, B., and Schmid, S. M., 2003, Late stages of deformation and exhumation of an orogen constrained by fission-track data: A case study in the Western Alps: Geological Society of America Bulletin, v. 115, n. 11, p. 1425–1440, http://dx.doi.org/10.1130/B25092.1
Fügenschuh, B., Seward, D., and Mancktelow, N., 1997, Exhumation in a convergent orogen: The western Tauern window: Terra Nova, v. 9, n. 5–6, p. 213–217, http://dx.doi.org/10.1111/j.1365-3121.1997.tb00015.x
Fügenschuh, B., Loprieno, A., Ceriani, S., and Schmid, S. M., 1999, Structural analysis of the Subbriançonnais and Valais units in the area of Moûtiers (Savoy, Western Alps): Paleogeographic and tectonic consequences: International Journal of Earth Sciences, v. 88, n. 2, p. 201–218, http://dx.doi.org/10.1007/s005310050260
Gallagher, K., Brown, R., and Johnson, C., 1998, Fission track analysis and its applications to geological

problems: Annual Review of Earth and Planetary Sciences, v. 26, n. 1, p. 519–572, http://dx.doi.org/10.1146/annurev.earth.26.1.519

Garver, J. I., Brandon, M. T., Roden-Tice, M., and Kamp, P. J. J., 1999, Exhumation history of orogenic highlands determined by detrital fission-track thermochronology, *in* Ring, U., Brandon, M. T., Lister, G. S., and Willett, S. A., editors, Exhumation Processes-Normal Faulting, Ductile Flow and Erosion: Geological Society, London, Special Publications, v. 154, p. 283–304, http://dx.doi.org/10.1144/GSL.SP.1999.154.01.13

Gerlach, H., 1869, Die Penninishen Alpen: Denkschrift Schweizer Naturforschendes, v. 23, p. 1–68.

Gerner, P., Bada, G., Dövényi, P., Müller, B., Oncescu, M. C., Cloetingh, S., and Horváth, F., 1999, Recent tectonic stress and crustal deformation in and around the Pannonian Basin: Data and models, *in* Durand, B., Jolivet, L., Horvath, F., and Seranne, M., editors, The Mediterranean Basins-Tertiary Extension within the Alpine Orogen: Geological Society, London, Special Publications, v. 156, p. 269–294, http://dx.doi.org/10.1144/GSL.SP.1999.156.01.14

Giger, M., ms, 1991, Geochronologische und petrographische Studien an Geröllen und Sedimenten der Gonfolite Lombarda Gruppe (Südschweiz und Norditalien) und ihr Vergleich mit dem alpinen Hinterland: Bern, Switzerland, University of Bern, Ph. D. thesis, 230 p.

Glotzbach, C., Reinecker, J., Danišík, M., Rahn, M., Frisch, W., and Spiegel, C., 2008, Neogene exhumation history of the Mont Blanc massif, Western Alps: Tectonics, v. 27, n. 4, TC4011, http://dx.doi.org/10.1029/2008TC002257

Glotzbach, C., Spiegel, C., Reinecker, J., Rahn, M., and Frisch, W., 2009, What perturbs isotherms? An assessment using fission-track thermochronology and thermal modelling along the Gotthard transect, Central Alps, *in* Lisker, F., Ventura, B., and Glasmacher, U. A., editors, Thermochronological Methods: From Paleotemperature Constraints to Landscape Evolution Models: Geological Society, London, Special Publications, v. 324, p. 111, http://dx.doi.org/10.1144/SP324.9

Glotzbach, C., Reinecker, J., Danišík, M., Rahn, M., Frisch, W., and Spiegel, C., 2010, Thermal history of the central Gotthard and Aar massifs, European Alps: Evidence for steady state, long-term exhumation: Journal of Geophysical Research-Earth Surface, v. 115, n. F3, F03017, http://dx.doi.org/10.1029/2009JF001304

Glotzbach, C., van der Beek, P. A., and Spiegel, C., 2011, Episodic exhumation and relief growth in the Mont Blanc massif, Western Alps from numerical modelling of thermochronology data: Earth and Planetary Science Letters, v. 304, n. 3–4, p. 417–430, http://dx.doi.org/10.1016/j.epsl.2011.02.020

Grasemann, B., and Mancktelow, N. S., 1993, Two-dimensional thermal modelling of normal faulting: the Simplon Fault Zone, Central Alps, Switzerland: Tectonophysics, v. 225, n. 3, p. 155–165, 10.1016/0040-1951(93)90277-Q

Grove, M., and Harrison, T. M., 1996, ^{40}Ar* diffusion in Fe-rich biotite: American Mineralogist, v. 81, n. 7–8, p. 940.

Grundmann, G., and Morteani, G., 1985, The young uplift and thermal history of the Central Eastern Alps (Austria/Italy), evidence from apatite fission track ages: Jahrbruch Geologisches Bundesanst, v. 128, p. 197–216.

Haeuselmann, P., Granger, D. E., Jeannin, P. Y., and Lauritzen, S. E., 2007, Abrupt glacial valley incision at 0. 8 Ma dated from cave deposits in Switzerland: Geology, v. 35, n. 2, p. 143–147, http://dx.doi.org/10.1130/G23094A

Hales, T. C., and Roering, J. J., 2009, A frost "buzzsaw" mechanism for erosion of the eastern Southern Alps, New Zealand: Geomorphology, v. 107, n. 3–4, p. 241–253, http://dx.doi.org/10.1016/j.geomorph.2008.12.012

Hames, W. E., and Bowring, S. A., 1994, An empirical evaluation of the argon diffusion geometry in muscovite: Earth and Planetary Science Letters, v. 124, n. 1–4, p. 161–169, http://dx.doi.org/10.1016/0012-821X(94)00079-4

Handy, M. R., Schmid, S. M., Bousquet, R., Kissling, E., and Bernoulli, D., 2010, Reconciling plate-tectonic reconstructions of Alpine Tethys with the geological-geophysical record of spreading and subduction in the Alps: Earth-Science Reviews, v. 102, n. 3–4, 121–158, http://dx.doi.org/10.1016/j.earscirev.2010.06.002

Harbor, J. M., Hallet, B., and Raymond, C. F., 1988, A numerical model of landform development by glacial erosion: Nature, v. 333, p. 347–349, http://dx.doi.org/10.1038/333347a0

Hay, W. W., Sloan, J. L., II, and Wold, C. N., 1988, Mass/age distribution and composition of sediments on the ocean floor and the global rate of sediment subduction: Journal of Geophysical Research-Solid Earth, v. 93, n. B12, p. 14933–14940, http://dx.doi.org/10.1029/JB093iB12p14933

Hejl, E., 1997, 'Cold spots' during the Cenozoic evolution of the Eastern Alps: Thermochronological interpretation of apatite fission-track data: Tectonophysics, v. 272, n. 2–4, p. 159–173, http://dx.doi.org/10.1016/S0040-1951(96)00256-9

Hejl, E., and Grundmann, G., 1989, Apatit-Spaltspurendaten zur thermischen Geschichte der Nördlichen Kalkalpen, der Flysch-und Molassezone: Vienna, Jahrbuch der Geologischen Bundesanstalt, v. 132, p. 191–212.

Herwartz, D., Nagel, T. J., Münker, C., Scherer, E. E., and Froitzheim, N., 2011, Tracing two orogenic cycles in one eclogite sample by Lu–Hf garnet chronometry: Nature Geoscience, v. 4, n. 3, p. 178–183, http://dx.doi.org/10.1038/ngeo1060

Hetherington, C. J., and Villa, I. M., 2007, Barium silicates of the Berisal Complex, Switzerland: A study in geochronology and rare-gas release systematics: Geochimica et Cosmochimica Acta, v. 71, n. 13, p. 3336–3347, http://dx.doi.org/10.1016/j.gca.2007.05.001

Hindle, D., 2008, How hard were the Jura mountains pushed?: Swiss Journal of Geosciences, v. 101, n. 2, p. 305–310, http://dx.doi.org/10.1007/s00015-008-1272-2

Homewood, P., Allen, P., and Williams, G., 1986, Dynamics of the Molasse Basin of western Switzerland: Foreland Basins, v. 8, p. 199–217, http://dx.doi.org/10.1002/9781444303810.ch10

Horváth, F., and Cloetingh, S., 1996, Stress-induced late-stage subsidence anomalies in the Pannonian basin: Tectonophysics, v. 266, n. 1–4, p. 287–300, http://dx.doi.org/10.1016/S0040-1951(96)00194-1

Howard, A. D., and Kerby, G., 1983, Channel changes in badlands: Bulletin of the Geological Society of America, v. 94, n. 6, p. 739–752, http://dx.doi.org/10.1130/0016-7606(1983)94<739:CCIB>2.0.CO;2

Hunziker, J. C., 1970, Polymetamorphism in the Monte Rosa, Western Alps: Eclogae Geologicae Helvetiae, v. 63, p. 151–161.

Hunziker, J. C., and Bearth, P., 1969, Rb-Sr-Altersbestimmungen aus den Walliser Alpen. Biotitalterswerte und ihre Bedeutung für die Abkühlungsgeschichte der alpinen Metamorphose: Eclogae Geologicae Helvetiae, v. 62, p. 205–222.

Hunziker, J. C., Desmons, J., and Hurford, A., 1992, Thirty-two years of geochronological work in the Central and Western Alps: A review on seven maps: Lausanne, Mémoires de Géologie, v. 13, p. 1–59.

Hurford, A. J., 1986, Cooling and uplift patterns in the Lepontine Alps South Central Switzerland and an age of vertical movement on the Insubric fault line: Contributions to Mineralogy and Petrology, v. 92, n. 4, p. 413–427, http://dx.doi.org/10.1007/BF00374424

Hurford, A. J., and Hunziker, J. C., 1985, Alpine cooling history of the Monte Mucrone eclogites (Sesia-Lanzo zone): Fission track evidence: Schweizerische Mineralogische und Petrographische Mitteilungen, v. 65, n. 2–3, p. 325–334.

——— 1989, A revised thermal history for the Gran Paradiso massif: Schweizerische Mineralogische und Petrographische Mitteilungen, v. 69, p. 319–329.

Hurford, A., Flisch, M., and Jäger, E., 1989, Unravelling the thermo-tectonic evolution of the Alps: A contribution from fission track analysis and mica dating: Geological Society, London, Special Publications, v. 45, p. 369–398, http://dx.doi.org/10.1144/GSL.SP.1989.045.01.21

Hurford, A. J., Hunziker, J. C., and Stöckhert, B., 1991, Constraints on the late thermotectonic evolution of the western Alps: Evidence for episodic rapid uplift: Tectonics, v. 10, n. 4, p. 758–769, http://dx.doi.org/10.1029/91TC00167

Jackson, D. D., 1972, Interpretation of Inaccurate, Insufficient and Inconsistent Data: Geophysical Journal of the Royal Astronomical Society, v. 28, n. 2, p. 97–109, http://dx.doi.org/10.1111/j.1365-246X.1972.tb06115.x

Jäger, E., and Faul, H., 1959, Age measurements on some granites and gneisses from the Alps: Geological Society of America Bulletin, v. 70, n. 12, p. 1553–1558, http://dx.doi.org/10.1130/0016-7606(1959)70[1553:AMOSGA]2.0.CO;2

Janots, E., Engi, M., Rubatto, D., Berger, A., Gregory, C., and Rahn, M., 2009, Metamorphic rates in collisional orogeny from *in situ* allanite and monazite dating: Geology, v. 37, n. 1, p. 11–14, http://dx.doi.org/10.1130/G25192A.1

Jarvis, A., Reuter, H. I., Nelson, A., and Guevara, E., 2006, Void-filled seamless SRTM data V3, available from the CGIAR-CSI SRTM 90m Database: http://srtm. csi. cgiar. org

Jenkin, G. R. T., 1997, Do cooling paths derived from mica Rb-Sr data reflect true cooling paths?: Geology, v. 25, n. 10, p. 907, http://dx.doi.org/10.1130/0091-7613(1997)025<0907:DCPDFM>2.3.CO;2

Karner, G. D., and Watts, A. B., 1983, Gravity anomalies and flexure of the lithosphere at mountain ranges: Journal of Geophysical Research-Solid Earth, v. 88, n. B12, p. 10449–10477, http://dx.doi.org/10.1029/JB088iB12p10449

Keller, L. M., Abart, R., Schmid, S. M., and De Capitani, C., 2005, Phase relations and chemical composition of phengite and paragonite in pelitic schists during decompression: A case study from the Monte Rosa nappe and Camughera–Moncucco unit, Western Alps: Journal of Petrology, v. 46, n. 10, p. 2145, http://dx.doi.org/10.1093/petrology/egi051

Kempf, O., Matter, A., Burbank, D. W., and Mange, M., 1999, Depositional and structural evolution of a foreland basin margin in a magnetostratigraphic framework: The eastern Swiss Molasse Basin: International Journal of Earth Sciences, v. 88, n. 2, p. 253–275, http://dx.doi.org/10.1007/s005310050263

Ketcham, R. A., Donelick, R. A., and Carlson, W. D., 1999, Variability of apatite fission-track annealing kinetics: III. Extrapolation to geological time scales: American Mineralogist, v. 84, n. 9, p. 1235–1255, http://dx.doi.org/10.2138/am-1999-0903

Kissling, E., 1993, Deep structure of the Alps–what do we really know?: Physics of the Earth and Planetary Interiors, v. 79, n. 1–2, p. 87–112, http://dx.doi.org/10.1016/0031-9201(93)90144-X

——— 2008, Deep structure and tectonics of the Valais and the rest of the Alps: Bulletin fuer Angewandte Geologie, v. 13, n. 2, p. 3–10.

Kissling, E., Schmid, S. M., Lippitsch, R., Ansorge, J., and Fügenschuh, B., 2006, Lithosphere structure and tectonic evolution of the Alpine arc: New evidence from high-resolution teleseismic tomography: Geological Society, London, Memoirs, v. 32, p. 129, http://dx.doi.org/10.1144/GSL.MEM.2006.032.01.08

Knaus, A., ms, 1990, Apatit-Spaltspurendatierungen in Rätikon (Arosazone, Östalpen): Tübingen, Germany, University of Tübingen, Ph. D. thesis, 60 p.

Korup, O., and Schlunegger, F., 2009, Rock-type control on erosion-induced uplift, eastern Swiss Alps: Earth and Planetary Science Letters, v. 278, n. 3–4, p. 278–285, http://dx.doi.org/10.1016/j.epsl.2008.12.012

Kuhlemann, J., 2000, Post-collisional sediment budget of circum-Alpine basins (Central Europe): Memorie degli Istituti di Geolgia e Mineralogia dell' Universita di Padova, v. 52, n. 1, p. 1–91.

——— 2007, Paleogeographic and paleotopographic evolution of the Swiss and Eastern Alps since the Oligocene: Global and Planetary Change, v. 58, n. 1–4, p. 224–236, http://dx.doi.org/10.1016/j.gloplacha.2007.03.007

Kuhlemann, J., and Kempf, O., 2002, Post-Eocene evolution of the North Alpine Foreland Basin and its

response to Alpine tectonics: Sedimentary Geology, v. 152, n. 1–2, p. 45–78, http://dx.doi.org/10.1016/S0037-0738(01)00285-8
Kuhlemann, J., Frisch, W., Dunkl, I., and Székely, B., 2001, Quantifying tectonic versus erosive denudation by the sediment budget: The Miocene core complexes of the Alps: Tectonophysics, v. 330, n. 1–2, p. 1–23, http://dx.doi.org/10.1016/S0040-1951(00)00209-2
Kuhlemann, J., Frisch, W., Székely, B., Dunkl, I., and Kázmér, M., 2002, Post-collisional sediment budget history of the Alps: Tectonic versus climatic control: International Journal of Earth Sciences, v. 91, n. 5, p. 818–837, http://dx.doi.org/10.1007/s00531-002-0266-y
Kuhlemann, J., Dunkl, I., Brugel, A., Spiegel, C., and Frisch, W., 2006, From source terrains of the Eastern Alps to the Molasse Basin: Detrital record of non-steady-state exhumation: Tectonophysics, v. 413, n. 3–4, p. 301–316, http://dx.doi.org/10.1016/j.tecto.2005.11.007
Kühni, A., and Pfiffner, O., 2001, The relief of the Swiss Alps and adjacent areas and its relation to lithology and structure: Topographic analysis from a 250-m DEM: Geomorphology, v. 41, n. 4, p. 285–307, http://dx.doi.org/10.1016/S0169-555X(01)00060-5
Lelarge, L., 1993, ms, Thermochronologie par la méthode des traces de fission d'une marge passive (Dome de Ponta Grossa, SE Brésil) et au sein d'une cha'5eıne de collision (zone externe de l'arc alpin, France): Grenoble, France, University of Grenoble, Ph. D. thesis, 145 p.
Leloup, P. H., Arnaud, N., Sobel, E. R., and Lacassin, R., 2005, Alpine thermal and structural evolution of the highest external crystalline massif: The Mont Blanc: Tectonics, v. 24, n. 4, TC4002, http://dx.doi.org/10.1029/2004TC001676
Lihou, J., Hurford, A., and Carter, A., 1995, Preliminary fission-track ages on zircons and apatites from the Sardona unit, Glarus Alps, eastern Switzerland: Late Miocene-Pliocene exhumation rates: Schweizerische Mineralogische und Petrographische Mitteilungen, v. 75, p. 177–186.
Lippitsch, R., Kissling, E., and Ansorge, J., 2003, Upper mantle structure beneath the Alpine orogen from high-resolution teleseismic tomography: Journal of Geophysical Research- Solid Earth, v. 108, n. B8, http://dx.doi.org/10.1029/2002JB002016
Lucazeau, F., and Vasseur, G., 1989, Heat flow density data from France and surrounding margins: Tectonophysics, v. 164, n. 2–4, p. 251–258, http://dx.doi.org/10.1016/0040-1951(89)90018-8
Lugeon, M., 1914, Sur l'ampleur de la Nappe de Morcles: Comptes Rendus de l'Académie des Sciences, Paris, v. 158, p. 2029–2030.
Luth, S. W., and Willingshofer, E., 2008, Mapping of the post-collisional cooling history of the Eastern Alps: Swiss Journal of Geosciences, v. 101, Supplement 1, p. 207–223, http://dx.doi.org/10.1007/s00015-008-1294-9
Lyon-Caen, H., and Molnar, P., 1989, Constraints on the deep structure and dynamic processes beneath the Alps and adjacent regions from an analysis of gravity anomalies: Geophysical Journal International, v. 99, n. 1, p. 19–32, http://dx.doi.org/10.1111/j.1365-246X.1989.tb02013.x
Madritsch, H., Preusser, F., Fabbri, O., Bichet, V., Schlunegger, F., and Schmid, S. M., 2010, Late Quaternary folding in the Jura Mountains: Evidence from syn-erosional deformation of fluvial meanders: Terra Nova, v. 22, n. 2, p. 147–154, http://dx.doi.org/10.1111/j.1365-3121.2010.00928.x
Mahéo, G., Gautheron, C., Leloup, P.-H., Fox, M., Tassant-Got, L., and Douville, E., 2012, Neogene exhumation history of the Bergell massif (southeast Central Alps): Terra Nova, v. 25, n. 2, p. 110–118, http://dx.doi.org/10.1111/ter.12013
Malusà, M. G., Polino, R., Zattin, M., Bigazzi, G., Martin, S., and Piana, F., 2005, Miocene to Present differential exhumation in the Western Alps: Insights from fission track thermochronology: Tectonics, v. 24, n. 3, TC3004, http://dx.doi.org/10.1029/2004TC001782
Mancktelow, N. S., 1992, Neogene lateral extension during convergence in the Central Alps: Evidence from interrelated faulting and backfolding around the Simplonpass (Switzerland): Tectonophysics, v. 215, n. 3–4, p. 295–317, http://dx.doi.org/10.1016/0040-1951(92)90358-D
Mancktelow, N. S., and Grasemann, B., 1997, Time-dependent effects of heat advection and topography on cooling histories during erosion: Tectonophysics, v. 270, n. 3–4, p. 167–195, http://dx.doi.org/10.1016/S0040-1951(96)00279-X
Marchant, R., ms, 1993, The Underground of the Western Alps: Lausanne, Switzerland, Université de Lausanne, Ph. D. thesis, Mémoires de Géologie, n. 15, 147 p.
Markley, M. J., Teyssier, C., Cosca, M. A., Caby, R., Hunziker, J. C., and Sartori, M., 1998, Alpine deformation and ^{40}Ar/^{39}Ar geochronology of synkinematic white mica in the Siviez-Mischabel Nappe, western Pennine Alps, Switzerland: Tectonics, v. 17, n. 3, p. 407–425, http://dx.doi.org/10.1029/98TC00560
Martin, S., Bigazzi, G., Zattin, M., Viola, G., and Balestrieri, M. L., 1998, Neogene kinematics of the Giudicarie fault (Central-Eastern Alps, Italy): New apatite fission-track data: Terra Nova, v. 10, n. 4, p. 217–221, http://dx.doi.org/10.1046/j.1365-3121.1998.00119.x
Meyre, C., Marquer, D. S., Schmid, S. M., and Ciancaleoni, L., 1998, Syn-orogenic extension along the Forcola fault: Correlation of Alpine deformations in the Tambo and Adula nappes (Eastern Penninic Alps): Eclogae Geologicae Helvetiae, v. 91, n. 3, p. 409–420.
Michalski, I., and Soom, M., 1990, The Alpine thermo-tectonic evolution of the Aar and Gotthard massifs, central Switzerland: Fission track ages on zircon and apatite and K-Ar mica ages: Schweizerische Mineralogische und Petrographische Mitteilungen, v. 70, p. 373–387.
Mitterbauer, U., Behm, M., Brückl, E., Lippitsch, R., Guterch, A., Keller, G. R., Koslovskaya, E., Rumpfhuber, E.-M., and Šumanovac, F., 2011, Shape and origin of the East-Alpine slab constrained by the ALPASS teleseismic model: Tectonophysics, v. 510, n. 1–2, p. 195–206, http://dx.doi.org/10.1016/j.tecto.2011.07.001
Molnar, P., 2004, Late Cenozoic increase in accumulation rates of terrestrial sediment: How might climate change have affected erosion rates?: Annual Review of Earth and Planetary Sciences, v. 32, p. 67–89, http://dx.doi.org/10.1146/annurev.earth.32.091003.143456

Most, P., ms, 2003, Late Alpine cooling histories of tectonic blocks along the central part of the Transalp-Traverse (Inntal-Gadertal): Constraints from geochronology: Tübingen, Germany, University of Tübingen, Ph. D. thesis, 151 p.
Mugnier, J. L., and Vialon, P., 1986, Deformation and displacement of the Jura cover on its basement: Journal of Structural Geology, v. 8, n. 3–4, p. 373–387, http://dx.doi.org/10.1016/0191-8141(86)90056-8
Muttoni, G., Carcano, C., Garzanti, E., Ghielmi, M., Piccin, A., Pini, R., Rogledi, S., and Sciunnach, D., 2003, Onset of major Pleistocene glaciations in the Alps: Geology, v. 31, n. 11, p. 989–992, http://dx.doi.org/10.1130/G19445.1
Nicolas, A., Hirn, A., Nicolich, R., and Polino, R., 1990, Lithospheric wedging in the western Alps inferred from the ECORS-CROP traverse: Geology, v. 18, n. 7, p. 587, http://dx.doi.org/10.1130/0091-7613(1990)018<0587:LWITWA>2.3.CO;2
Nocquet, J. M., and Calais, E., 2004, Geodetic measurements of crustal deformation in the Western Mediterranean and Europe: Pure and Applied Geophysics, v. 161, n. 3, p. 661–681, http://dx.doi.org/10.1007/s00024-003-2468-z
Peresson, H., and Decker, K., 1997, Far-field effects of Late Miocene subduction in the Eastern Carpathians: EW compression and inversion of structures in the Alpine-Carpathian-Pannonian region: Tectonics, v. 16, n. 1, p. 38–56, http://dx.doi.org/10.1029/96TC02730
Persaud, M., and Pfiffner, O. A., 2004, Active deformation in the eastern Swiss Alps: Post-glacial faults, seismicity and surface uplift: Tectonophysics, v. 385, n. 1–4, p. 59–84, http://dx.doi.org/10.1016/j.tecto.2004.04.020
Pfiffner, A., 1992, Alpine orogeny, *in* Blundell, D., Freeman, R., and Mueller, S., editors, A Continent Revealed: The European Geotraverse: Cambridge, England, Cambridge University Press, p. 180–190.
——— 1993, The structure of the Helvetic nappes and its relation to the mechanical stratigraphy: Journal of Structural Geology, v. 15, n. 3, p. 511–521, http://dx.doi.org/10.1016/0191-8141(93)90145-Z
Pfiffner, O. A., Frei, W., Valasek, P., Stäuble, M., Levato, L., Dubois, L., Schmid, S. M., and Smithson, S. B., 1990, Crustal shortening in the Alpine Orogen: Results from deep seismic reflection profiling in the eastern Swiss Alps, Line NFP 20-east: Tectonics, v. 9, n. 6, p. 1327–1355, http://dx.doi.org/10.1029/TC009i006p01327
Pfiffner, O. A., Schlunegger, F., and Buiter, S. J. H., 2002, The Swiss Alps and their peripheral foreland basin: Stratigraphic response to deep crustal processes: Tectonics, v. 21, n. 2, p. 1009, http://dx.doi.org/10.1029/2000TC900039
Pignalosa, A., Zattin, M., Massironi, M., and Cavazza, W., 2011, Thermochronological evidence for a late Pliocene climate-induced erosion rate increase in the Alps: International Journal of Earth Sciences, v. 100, n. 4, p. 847–859, http://dx.doi.org/10.1007/s00531-010-0510-9
Plan, L., Grasemann, B., Spötl, C., Decker, K., Boch, R., and Kramers, J., 2010, Neotectonic extrusion of the Eastern Alps: Constraints from U/Th dating of tectonically damaged speleothems: Geology, v. 38, n. 6, p. 483–486, http://dx.doi.org/10.1130/G30854.1
Purdy, J. W., and Jäger, E., 1976, K-Ar ages on rock-forming minerals from the Central Alps: Memorie degli Instituti di Geologia e Mineralogia dell' Universitá di Padova, v. 30, p. 1–32.
Rahn, M. K., Hurford, A. J., and Frey, M., 1997, Rotation and exhumation of a thrust plane: Apatite fission-track data from the Glarus thrust, Switzerland: Geology, v. 25, n. 7, p. 599–602, http://dx.doi.org/10.1130/0091-7613(1997)025<0599:RAEOAT>2.3.CO;2
Ramsay, J., 1981, Tectonics of the Helvetic nappes, *in* McClay, K. R., and Price, N. J., editors, Thrust and Nappe Tectonics: Geological Society, London, Special Publications, v. 9, p. 293–309, http://dx.doi.org/10.1144/GSL.SP.1981.009.01.26
Ratschbacher, L., Frisch, W., Linzer, H. G., and Merle, O., 1991a, Lateral extrusion in the Eastern Alps, Part 2: Structural analysis: Tectonics, v. 10, n. 2, p. 257–271, http://dx.doi.org/10.1029/90TC02623
Ratschbacher, L., Merle, O., Davy, P., and Cobbold, P., 1991b, Lateral extrusion in the Eastern Alps, Part 1: Boundary conditions and experiments scaled for gravity: Tectonics, v. 10, n. 2, p. 245–256, http://dx.doi.org/10.1029/90TC02622
Reinecker, J., Danišík, M., Schmid, C., Glotzbach, C., Rahn, M., Frisch, W., and Spiegel, C., 2008, Tectonic control on the late stage exhumation of the Aar Massif (Switzerland): Constraints from apatite fission track and (U-Th)/He data: Tectonics, v. 27, n. 6, TC6009, http://dx.doi.org/10.1029/2007TC002247
Reiners, P. W., and Brandon, M. T., 2006, Using thermochronology to understand orogenic erosion: Annual Review of Earth and Planetary Sciences, v. 34, p. 419–466, http://dx.doi.org/10.1146/annurev.earth.34.031405.125202
Reiners, P. W., Spell, T. L., Nicolescu, S., and Zanetti, K. A., 2004, Zircon (U-Th)/He thermochronometry: He diffusion and comparisons with $^{40}Ar/^{39}Ar$ dating: Geochimica et Cosmochimica Acta, v. 68, n. 8, p. 1857–1887, http://dx.doi.org/10.1016/j.gca.2003.10.021
Reverman, R. L., Fellin, M. G., Herman, F., Willett, S. D., and Fitoussi, C., 2012, Climatically versus tectonically forced erosion in the Alps: Thermochronometric constraints from the Adamello Complex, Southern Alps, Italy: Earth and Planetary Science Letters, v. 339–340, p. 127–138, http://dx.doi.org/10.1016/j.epsl.2012.04.051
Ring, U., Brandon, M. T., Willett, S. D., and Lister, G. S., 1999, Exhumation processes, *in* Ring, U., Brandon, M. T., Lister, G. S., and Willett, S. D., editors, Exhumation Processes: Normal Faulting, Ductile Flow and Erosion: Geological Society, London, Special Publications, v. 154, n. 1, p. 1–27, http://dx.doi.org/10.1144/GSL.SP.1999.154.01.01
Roe, G. H., Montgomery, D. R., and Hallet, B., 2003, Orographic precipitation and the relief of mountain ranges: Journal of Geophysical Research-Solid Earth, v. 108, n. B6, 2315, http://dx.doi.org/10.1029/2001JB001521
Roe, G. H., Whipple, K. X., and Fletcher, J. K., 2008, Feedbacks among climate, erosion, and tectonics in a

critical wedge orogen: American Journal of Science, v. 308, n. 7, p. 815–842, http://dx.doi.org/10.2475/07.2008.01
Romer, R. L., Schärer, U., and Steck, A., 1996, Alpine and pre-Alpine magmatism in the root-zone of the western Central Alps: Contributions to Mineralogy and Petrology, v. 123, n. 2, p. 138–158 http://dx.doi.org/10.1007/s004100050147
Rosenberg, C. L., and Berger, A., 2009, On the causes and modes of exhumation and lateral growth of the Alps: Tectonics, v. 28, n. 6, TC6001, http://dx.doi.org/10.1029/2008TC002442
Rosenberg, C. L., Brun, J. P., Cagnard, F., and Gapais, D., 2007, Oblique indentation in the Eastern Alps: Insights from laboratory experiments: Tectonics, v. 26, n. 2, TC2003, http://dx.doi.org/10.1029/2006TC001960
Roure, F., Polino, R., and Nicolich, R., 1990, Early Neogene deformation beneath the Po plain: Constraints on the post-collisional Alpine evolution: Mémoires de la Société géologique de France, v. 156, p. 309–321.
Rubatto, D., Regis, D., Hermann, J., Boston, K., Engi, M., Beltrando, M., and McAlpine, S. R. B., 2011, Yo–yo subduction recorded by accessory minerals in the Italian Western Alps: Nature Geoscience, v. 4, n. 5, p. 338–342, http://dx.doi.org/10.1038/ngeo1124
Sabil, N., ms, 1994, La datation par traces de fission: aspects méthodologiques et applications thermochronologiques en contextes alpins et de marge continentale: Grenoble, France, University of Grenoble, Ph. D. thesis, 238 p.
Sadler, P. M., 1999, The influence of hiatuses on sediment accumulation rates: GeoResearch Forum, v. 5, p. 15–40.
Sanchez, G., Rolland, Y., Jolivet, M., Brichau, S., Corsini, M., and Carter, A., 2011, Exhumation controlled by transcurrent tectonics: The Argentera-Mercantour massif (SW Alps): Terra Nova, v. 23, n. 2, p. 116–126, http://dx.doi.org/10.1111/j.1365-3121.2011.00991.x
Sanders, C. A. E., Andriessen, P. A. M., and Cloetingh, S. A. P. L., 1999, Life cycle of the East Carpathian orogen: Erosion history of a doubly vergent critical wedge assessed by fission track thermochronology: Journal of Geophysical Research, v. 104, n. B12, p. 29095–29112, http://dx.doi.org/10.1029/1998JB900046
Schaer, J. P., Reimer, G. M., and Wagner, G. A., 1975, Actual and ancient uplift rate in the Gotthard region, Swiss Alps: A comparison between precise levelling and fission-track apatite age: Tectonophysics, v. 29, n. 1–4, p. 293–300, http://dx.doi.org/10.1016/0040-1951(75)90154-7
Scharf, A., Handy, M. R., Ziemann, M. A., and Schmid, S. M., 2013, Peak-temperature patterns of polyphase metamorphism resulting from accretion, subduction and collision (eastern Tauern Window, European Alps)–a study with Raman microspectroscopy on carbonaceous material (RSCM): Journal of Metamorphic Geology, v. 31, n. 8, p. 863–880, http://dx.doi.org/10.1111/jmg.12048
Schlatter, A., Schneider, D., Geiger, A., and Kahle, H. G., 2005, Recent vertical movements from precise levelling in the vicinity of the city of Basel, Switzerland: International Journal of Earth Sciences, v. 94, n. 4, p. 507–514, http://dx.doi.org/10.1007/s00531-004-0449-9
Schlunegger, F., and Hinderer, M., 2001, Crustal uplift in the Alps: Why the drainage pattern matters: Terra Nova, v. 13, n. 6, p. 425–432, http://dx.doi.org/10.1046/j.1365-3121.2001.00374.x
Schlunegger, F., and Simpson, G., 2002, Possible erosional control on lateral growth of the European Central Alps: Geology, v. 30, n. 10, p. 907–910, http://dx.doi.org/10.1130/0091-7613(2002)030<0907:PECOLG>2.0.CO;2
Schlunegger, F., and Willett, S. D., 1999, Spatial and temporal variations in exhumation of the central Swiss Alps and implications for exhumation mechanisms: Geological Society, London, Special Publications, v. 154, n. 1, p. 157–179, http://dx.doi.org/10.1144/GSL.SP.1999.154.01.07
Schlunegger, F., Jordan, T. E., and Klaper, E. M., 1997, Controls of erosional denudation in the orogen on foreland basin evolution: The Oligocene central Swiss Molasse Basin as an example: Tectonics, v. 16, n. 5, p. 823–840, http://dx.doi.org/10.1029/97TC01657
Schmid, S. M., and Kissling, E., 2000, The arc of the western Alps in the light of geophysical data on deep crustal structure: Tectonics, v. 19, n. 1, p. 62–85, http://dx.doi.org/10.1029/1999TC900057
Schmid, S. M., Aebli, H. R., Heller, F., and Zingg, A., 1989, The role of the Periadriatic Line in the tectonic evolution of the Alps: Geological Society, London, Special Publications, v. 45, p. 153–171, http://dx.doi.org/10.1144/GSL.SP.1989.045.01.08
Schmid, S. M., Pfiffner, O. A., Froitzheim, N., Schönborn, G., and Kissling, E., 1996, Geophysical-geological transect and tectonic evolution of the Swiss–Italian Alps: Tectonics, v. 15, n. 5, p. 1036–1064, http://dx.doi.org/10.1029/96TC00433
Schmid, S. M., Fügenschuh, B., Kissling, E., and Schuster, R., 2004, Tectonic map and overall architecture of the Alpine orogen: Eclogae Geologicae Helvetiae, v. 97, n. 1, p. 93–117, http://dx.doi.org/10.1007/s00015-004-1113-x
Schmid, S. M., Scharf, A., Handy, M. R., and Rosenberg, C. L., 2013, The Tauern Window (Eastern Alps, Austria): A new tectonic map, with cross-sections and a tectonometamorphic synthesis: Swiss Journal of Geosciences, v. 106, n. 1, n. 1–32, http://dx.doi.org/10.1007/s00015-013-0123-y
Schumer, R., and Jerolmack, D. J., 2009, Real and apparent changes in sediment deposition rates through time: Journal of Geophysical Research- Earth Surface, v. 114, n. F3, http://dx.doi.org/10.1029/2009JF001266
Schwartz, S., ms, 2000, La zone piémontaise des Alpes occidentales: un paléo-complexe de subduction. Arguments métamorphiques, géochronologiques et structuraux: Lyon, France, University of Lyon, Ph. D. thesis, 341 p.
Selverstone, J., 2005, Are the Alps Collapsing?: Annual Review of Earth and Planetary Sciences, v. 33, p. 113–132, http://dx.doi.org/10.1146/annurev.earth.33.092203.122535
Seward, D., and Mancktelow, N. S., 1994, Neogene kinematics of the central and western Alps: Evidence

from fission-track dating: Geology, v. 22, n. 9, p. 803–806, http://dx.doi.org/10.1130/0091-7613(1994)022<0803:NKOTCA>2.3.CO;2

Seward, D., Ford, M., Bürgisser, J., Lickorish, H., Williams, E., and Meckel, L., III, 1999, Preliminary results of fission-track analyses in the southern Pelvoux area, SE France, *in* Gosso, G., Jadoul, F., Sella, M., and Spalla, M. I., editors, Memoria del Institutio dell Geologia I Mineraligia di Universidad de Padova, Proceedings of 3rd Workshop on Alpine Geological Studies, Biella-Oropa, Italy, 29 September-October 1997: Memorie di Scienze Geologiche Padova, v. 51, p. 25–31.

Sinclair, H. D., 1997, Flysch to molasse transition in peripheral foreland basins: The role of the passive margin versus slab breakoff: Geology, v. 25, n. 12, p. 1123, http://dx.doi.org/10.1130/0091-7613(1997)025<1123:FTMTIP>2.3.CO;2

Singer, J., Diehl, T., Husen, S., Kissling, E., and Duretz, T., 2014, Alpine lithosphere slab rollback causing lower crustal seismicity in northern foreland: Earth and Planetary Science Letters, v. 397, p. 42–56, http://dx.doi.org/10.1016/j.epsl.2014.04.002

Snyder, N. P., Whipple, K. X., Tucker, G. E., and Merritts, D. J., 2000, Landscape response to tectonic forcing: Digital elevation model analysis of stream profiles in the Mendocino triple junction region, northern California: Bulletin of the Geological Society of America, v. 112, n. 8, p. 1250–1263, http://dx.doi.org/10.1130/0016-7606(2000)112<1250:LRTTFD>2.0.CO;2

Sommaruga, A., 1999, Décollement tectonics in the Jura foreland fold-and-thrust belt: Marine and Petroleum Geology, v. 16, n. 2, p. 111–134, http://dx.doi.org/10.1016/S0264-8172(98)00068-3

Soom, M. A., ms, 1990, Abkühlungs- und Hebungsgeschichte der Externmassive und der penninischen Decken beidseits der Simplon-Rhone-Linie seit dem Oligozän: Spaltspurdatierung and Apatit/Zirkon und K–Ar-Datierungen an Biotit/Muskovit (westliche Zentralalpen): Bern, Switzerland, University of Bern, Ph. D. thesis, 64 p.

Spiegel, C., Kuhlemann, J., Dunkl, I., Frisch, W., Von Eynatten, H., and Balogh, K., 2000, The erosion history of the Central Alps: Evidence from zircon fission track data of the foreland basin sediments: Terra Nova, v. 12, n. 4, p. 163–170, http://dx.doi.org/10.1046/j.1365-3121.2000.00289.x

Stampfli, G., and Marchant, R., 1997, Geodynamic evolution of the Tethyan margins of the Western Alps, *in* Pfiffner, O. A., Lehner, P., Heitzman, P. Z., Mueller, S., and Steck, A., editors, Deep structure of the Swiss Alps: Results from NRP, v. 20, p. 223–239.

Stampfli, G. M., and Marthaler, M., 1990, Divergent and convergent margins in the North-Western Alps confrontation to actualistic models: Geodinamica Acta, v. 4, n. 3, p. 159–184, http://dx.doi.org/10.1080/09853111.1990.11105208

Stampfli, G. M., Mosar, J., Marquer, D., Marchant, R., Baudin, T., and Borel, G., 1998, Subduction and obduction processes in the Swiss Alps: Tectonophysics, v. 296, n. 1–2, 159–204, http://dx.doi.org/10.1016/S0040-1951(98)00142-5

Staufenberg, H., 1987, Apatite fission-track evidence for postmetamorphic uplift and cooling history of the Eastern Tauern Window and the surrounding Austroalpine (Central Eastern Alps, Austria): Jahrbuch der Geolischen Bundesanstalt, v. 130, p. 571–586.

Steck, A., and Hunziker, J., 1994, The Tertiary structural and thermal evolution of the Central Alps–compressional and extensional structures in an orogenic belt: Tectonophysics, v. 238, n. 1–4, p. 229–254, http://dx.doi.org/10.1016/0040-1951(94)90058-2

Steenken, A., Siegesmund, S., Heinrichs, T., and Fügenschuh, B., 2002, Cooling and exhumation of the Rieserferner Pluton (Eastern Alps, Italy/Austria): International Journal of Earth Sciences, v. 91, n. 5, p. 799–817, http://dx.doi.org/10.1007/s00531-002-0260-4

Steiner, H., 1984, Mineralogisch-petrographische, geochemische und isotopengeologische Untersuchungen an einem Meta-Lamprophyr und seinem granodioritischen Nebengestein (Matorello-Gneis) aus der Maggia-Decke: Schweizerische Mineralogische und Petrographische Mitteilungen, v. 64, p. 227–259.

Sternai, P., Herman, F., Fox, M. R., and Castelltort, S., 2011, Hypsometric analysis to identify spatially variable glacial erosion: Journal of Geophysical Research-Earth Surface, v. 116, n. F3, F03001, http://dx.doi.org/10.1029/2010JF001823

Sternai, P., Herman, F., Champagnac, J.-D., Fox, M., Salcher, B., and Willett, S. D., 2012, Pre-glacial topography of the European Alps: Geology, v. 40, n. 12, p. 1067–1070, http://dx.doi.org/10.1130/G33540.1

Sternai, P., Herman, F., Valla, P. G., and Champagnac, J.-D., 2013, Spatial and temporal variations of glacial erosion in the Rhône valley (Swiss Alps): Insights from numerical modeling: Earth and Planetary Science Letters, v. 368, p. 119–131, http://dx.doi.org/10.1016/j.epsl.2013.02.039

Stockhert, B., Brix, M. R., Kleinschrodt, R., Hurford, A. J., and Wirth, R., 1999, Thermochronometry and microstructures of quartz–a comparison with experimental flow laws and predictions on the temperature of the brittle-plastic transition: Journal of Structural Geology, v. 21, n. 3, p. 351–369, http://dx.doi.org/10.1016/S0191-8141(98)00114-X

Stolar, D., Roe, G., and Willett, S. D., 2007, Controls on the patterns of topography and erosion rate in a critical orogen: Journal of Geophysical Research-Earth Surface, v. 112, n. F4, p. 2156–2202, http://dx.doi.org/10.1029/2006JF000713

Stüwe, K., White, L., and Brown, R., 1994. The influence of eroding topography on steady-state isotherms. Application to fission track analysis: Earth and Planetary Science Letters, v. 124, n. 1–4, p. 63–74, http://dx.doi.org/10.1016/0012-821X(94)00068-9

Sue, C., Thouvenot, F., Fréchet, J., and Tricart, P., 1999, Widespread extension in the core of the western Alps revealed by earthquake analysis: Journal of Geophysical Research-Solid Earth, v. 104, n. B11, p. 25611–25622, http://dx.doi.org/10.1029/1999JB900249

Sue, C., Delacou, B., Champagnac, J.-D., Allanic, C., Tricart, P., and Burkhard, M., 2007, Extensional neotectonics around the bend of the Western/Central Alps: An overview: International Journal of Earth Sciences, v. 96, n. 6, p. 1101–1129, http://dx.doi.org/10.1007/s00531-007-0181-3

Tarantola, A., and Valette, B., 1982, Generalized nonlinear inverse problems solved using the least squares criterion: Reviews of Geophysics Space Physics, v. 20, n. 2, p. 219–232, http://dx.doi.org/10.1029/RG020i002p00219

Thomson, S. N., Brandon, M. T., Tomkin, J. H., Reiners, P. W., Vásquez, C., and Wilson, N. J., 2010, Glaciation as a destructive and constructive control on mountain building: Nature, v. 467, n. 7313, p. 313–317, http://dx.doi.org/10.1038/nature09365

Timar-Geng, Z., Grujic, D., and Rahn, M., 2004, Deformation at the Leventina-Simano nappe boundary, Central Alps, Switzerland: Eclogae Geologicae Helvetiae, v. 97, n. 2, p. 265–278, http://dx.doi.org/10.1007/s00015-004-1121-4

Trautwein, B., ms, 2000, Detritus provenance and thermal history of the Rhenodanubian flysch zone: mosaicstones for the reconstruction of the geodynamic evolution of the Eastern Alps: Tübingen, Germany, Institut und Museum für Geologie und Paläontologie der Universität Tübingen, Ph. D. thesis, 75 p.

Tricart, P., van der Beek, P., Schwartz, S., and Labrin, E., 2007, Diachronous late-stage exhumation across the western Alpine arc: Constraints from apatite fission-track thermochronology between the Pelvoux and Dora-Maira Massifs: Journal of the Geological Society, London, v. 164, n. 1, p. 163–174, http://dx.doi.org/10.1144/0016-76492005-174

Trümpy, R., 1973, The timing of orogenic events in the Central Alps, *in* De Jong, K., and Scholten, R., editors, Gravity and Tectonics: New York, Wiley, p. 229–251.

——— 1980, Geology of Switzerland, A guidebook: An outline of the geology of Switzerland: Basel, Switzerland, Schweiz Geol Komm, Wepf, 104 p.

——— 1988, A possible Jurassic-Cretaceous transform system in the Alps and the Carpathians: Geological Society of America Special Papers, v. 218, p. 93–109, http://dx.doi.org/10.1130/spe218-p93

Turcotte, D. L., and Schubert, G., 1982, Geodynamics applications of continuum physics to geological problems: New York, New York, John Wiley and Sons, Inc., 450 p.

Ustaszewski, K., and Schmid, S. M., 2007, Latest Pliocene to recent thick-skinned tectonics at the Upper Rhine Graben–Jura Mountains junction: Swiss Journal of Geosciences, v. 100, n. 2, p. 293–312, http://dx.doi.org/10.1007/s00015-007-1226-0

Ustaszewski, K., Schmid, S. M., Fügenschuh, B., Tischler, M., Kissling, E., and Spakman, W., 2008, A map-view restoration of the Alpine-Carpathian-Dinaridic system for the Early Miocene: Swiss Journal of Geosciences, v. 101, Supplement 1, p. 273–294, http://dx.doi.org/10.1007/s00015-008-1288-7

Valla, P. G., Shuster, D. L., and van der Beek, P. A., 2011, Significant increase in relief of the European Alps during mid-Pleistocene glaciations: Nature Geoscience, v. 4, n. 10, p. 688–692, http://dx.doi.org/10.1038/ngeo1242

Valla, P. G., van der Beek, P. A., Shuster, D. L., Braun, J., Herman, F., Tassan-Got, L., and Gautheron, C., 2012, Late Neogene exhumation and relief development of the Aar and Aiguilles Rouges massifs (Swiss Alps) from low-temperature thermochronology modeling and $^4He/^3He$ thermochronometry: Journal of Geophysical Research- Earth Surface, v. 117, n. F1, F01004, http://dx.doi.org/10.1029/2011JF002043

van der Beek, P. A., Valla, P. G., Herman, F., Braun, J., Persano, C., Dobson, K. J., and Labrin, E., 2010, Inversion of thermochronological age-elevation profiles to extract independent estimates of denudation and relief history–II: Application to the French Western Alps: Earth and Planetary Science Letters, v. 296, n. 1–2, p. 9–22, http://dx.doi.org/10.1016/j.epsl.2010.04.032

Vernon, A. J., van der Beek, P. A., Sinclair, H. D., and Rahn, M. K., 2008, Increase in late Neogene denudation of the European Alps confirmed by analysis of a fission-track thermochronology database: Earth and Planetary Science Letters, v. 270, n. 3–4, p. 316–329, http://dx.doi.org/10.1016/j.epsl.2008.03.053

Viola, G., ms, 2000, Kinematics and timing of the Periadriatic fault system in the Giudicarie region (central-Eastern Alps): Zürich, Switzerland, ETH Zürich, Ph. D. thesis, 206 p.

Viola, G., Mancktelow, N. S., and Seward, D., 2001, Late Oligocene-Neogene evolution of Europe-Adria collision: New structural and geochronological evidence from the Giudicarie fault system (Italian Eastern Alps): Tectonics, v. 20, n. 6, p. 999–1020, http://dx.doi.org/10.1029/2001TC900021

Viola, G., Mancktelow, N. S., Seward, D., Meier, A., and Martin, S., 2003, The Pejo fault system: An example of multiple tectonic activity in the Italian Eastern Alps: Geological Society of America Bulletin, v. 115, n. 5, p. 515, http://dx.doi.org/10.1130/0016-7606(2003)115<0515:TPFSAE>2.0.CO;2

von Blanckenburg, F., and Davies, J. H., 1995, Slab breakoff: A model for syncollisional magmatism and tectonics in the Alps: Tectonics, v. 14, n. 1, p. 120–131, http://dx.doi.org/10.1029/94TC02051

von Blanckenburg, F., Villa, I. M., Baur, H., Morteani, G., and Steiger, R., 1989, Time calibration of a PT-path from the Western Tauern Window, Eastern Alps: The problem of closure temperatures: Contributions to Mineralogy and Petrology, v. 101, n. 1, p. 1–11, http://dx.doi.org/10.1007/BF00387196

von Hagke, C., Cederbom, C. E., Oncken, O., Stöckli, D. F., Rahn, M. K., and Schlunegger, F., 2012, Linking the northern Alps with their foreland: The latest exhumation history resolved by low-temperature thermochronology: Tectonics, v. 31, n. 5, http://dx.doi.org/10.1029/2011TC003078

Wagner, G. A., and Reimer, G. M., 1972, Fission track tectonics: The tectonic interpretation of fission track apatite ages: Earth and Planetary Science Letters, v. 14, n. 2, p. 263–268, http://dx.doi.org/10.1016/0012-821X(72)90018-0

Wagner, G. A., Reimer, G., and Jäger, E., 1977, Cooling ages derived by apatite fission track, mica Rb-Sr and K-Ar dating: The uplift and cooling history of the Central Alps: Memorie degli Istituti di Geologia e Minalogia dell' Universitá di Padova, v. 30, p. 1–27.

Wagner, G. A., Miller, D. S., and Jäger, E., 1979, Fission track ages on apatite of Bergell rocks from Central

Alps and Bergell boulders in Oligocene sediments: Earth and Planetary Science Letters, v. 45, n. 2, p. 355–360, http://dx.doi.org/10.1016/0012-821X(79)90136-5
Weh, M., ms, 1998, Tektonische Entwicklung der penninischen Sediment-Decken in Graubünden (Prättigau bis Oberhalbstein): Basel, Switzerland, Ph.D. thesis, 230 p.
Werner, D., 1985, Geothermal problems in mountain ranges (Alps): Tectonophysics, v. 121, n. 1, p. 97–108, http://dx.doi.org/10.1016/0040-1951(85)90271-9
Wessel, P., and Smith, W. H. F., 1998, New, improved version of Generic Mapping Tools released: Eos Transactions, v. 79, n. 47, p. 579–579, http://dx.doi.org/10.1029/98EO00426
Whipple, K. X., and Meade, B. J., 2004, Controls on the strength of coupling among climate, erosion, and deformation in two-sided, frictional orogenic wedges at steady state: Journal of Geophysical Research-Earth Surface, v. 109, n. F1, p. 2156–2202, http://dx.doi.org/10.1029/2003JF000019
Whipple, K. X., and Tucker, G. E., 1999, Dynamics of the stream-power river incision model: Implications for height limits of mountain ranges, landscape response timescales, and research needs: Journal of Geophysical Research- Solid Earth, v. 104, n. B8, p. 17661–17674, http://dx.doi.org/10.1029/1999JB900120
Wiederkehr, M., Bousquet, R., Schmid, S. M., and Berger, A., 2008, From subduction to collision: Thermal overprint of HP/LT meta-sediments in the north-eastern Lepontine Dome (Swiss Alps) and consequences regarding the tectono-metamorphic evolution of the Alpine orogenic wedge: Swiss Journal of Geosciences, v. 101, Supplement 1, p. 127–155, http://dx.doi.org/10.1007/s00015-008-1289-6
Willenbring, J. K., and Von Blanckenburg, F., 2010, Long-term stability of global erosion rates and weathering during late-cenozoic cooling: Nature, v. 465, n. 7295, p. 211–214, http://dx.doi.org/10.1038/nature09044
Willett, S. D., 2010, Late Neogene erosion of the Alps: A climate driver?: Annual Review of Earth and Planetary Sciences, v. 38, p. 411–437, http://dx.doi.org/10.1146/annurev-earth-040809-152543
Willett, S. D., and Schlunegger, F., 2010, The last phase of depositioin in the Swiss Molasse Basin: From foredeep to negative alpha basin: Basin Research, v. 22, n. 5, p. 623–639, http://dx.doi.org/10.1111/j.1365-2117.2009.00435.x
Willett, S. D., Schlunegger, F., and Picotti, V., 2006, Messinian climate change and erosional destruction of the central European Alps: Geology, v. 34, n. 8, p. 613–617, http://dx.doi.org/10.1130/G22280.1
Wittmann, H., von Blanckenburg, F., Kruesmann, T., Norton, K. P., and Kubik, P. W., 2007, Relation between rock uplift and denudation from cosmogenic nuclides in river sediment in the Central Alps of Switzerland: Journal of Geophysical Research, v. 112, n. F04010, http://dx.doi.org/10.1029/2006jf000729
Wölfler, A., Dekant, C., Danišík, M., Kurz, W., Dunkl, I., Putiš, M., and Frisch, W., 2008, Late stage differential exhumation of crustal blocks in the central Eastern Alps: Evidence from fission track and (U–Th)/He thermochronology: Terra Nova, v. 20, n. 5, p. 378–384, http://dx.doi.org/10.1111/j.1365-3121.2008.00831.x
Wölfler, A., Kurz, W., Fritz, H., and Stüwe, K., 2011, Lateral extrusion in the Eastern Alps revisited: Refining the model by thermochronological, sedimentary, and seismic data: Tectonics, v. 30, n. 4, TC4006, http://dx.doi.org/10.1029/2010TC002782
Yanites, B. J., Ehlers, T. A., Becker, J. K., Schnellmann, M., and Heuberger, S., 2013, High magnitude and rapid incision from river capture: Rhine River, Switzerland: Journal of Geophysical Research: Earth Surface, v. 118, n. 2, p. 1060–1084, http://dx.doi.org/10.1002/jgrf.20056
Zattin, M., Stefani, C., and Martin, S., 2003, Detrital fission-track analysis and sedimentary petrofacies as keys of Alpine exhumation: The example of the Venetian Foreland (European Southern Alps, Italy): Journal of Sedimentary Research, v. 73, n. 6, p. 1051, http://dx.doi.org/10.1306/051403731051
Zattin, M., Cuman, A., Fantoni, R., Martin, S., Scotti, P., and Stefani, C., 2006, From Middle Jurassic heating to Neogene cooling: The thermochronological evolution of the southern Alps, *in* Gebrande, B., Castellarin, C., Lüschen, E., Neubauer, F., and Nicolich, R., editors, TRANSALP–A Transect Through a Young Collisional Orogen: Tectonophysics, v. 414, n. 1–4, p. 191–202, http://dx.doi.org/10.1016/j.tecto.2005.10.020
Zhang, P., Molnar, P., and Downs, W. R., 2001, Increased sedimentation rates and grain sizes 2-4 Myr ago due to the influence of climate change on erosion rates: Nature, v. 410, n. 6831, p. 891–897, http://dx.doi.org/10.1038/35073504